



Cite this: *Chem. Soc. Rev.*, 2015,  
 44, 3808

Received 15th January 2015

DOI: 10.1039/c5cs00038f

[www.rsc.org/csr](http://www.rsc.org/csr)

## Heterogeneous and homogeneous catalysis for the hydrogenation of carboxylic acid derivatives: history, advances and future directions

James Pritchard,<sup>†[a](#)</sup> Georgy A. Filonenko,<sup>†[ab](#)</sup> Robbert van Putten,<sup>[a](#)</sup> Emiel J. M. Hensen<sup>[ab](#)</sup> and Evgeny A. Pidko<sup>\*[ab](#)</sup>

The catalytic reduction of carboxylic acid derivatives has witnessed a rapid development in recent years. These reactions, involving molecular hydrogen as the reducing agent, can be promoted by heterogeneous and homogeneous catalysts. The milestone achievements and recent results by both approaches are discussed in this Review. In particular, we focus on the mechanistic aspects of the catalytic hydrogenation and highlight the bifunctional nature of the mechanism that is preferred for supported metal catalysts as well as homogeneous transition metal complexes.

### 1. Introduction

The hydrogenation of carboxylic acids and their esters (Scheme 1) is receiving increased attention in the context of upgrading of bio-based feedstocks. Seed and vegetable oils, which are important bio-based resources, can be transformed into fatty alcohols and other bulk chemicals.<sup>1–4</sup> Fatty alcohols

in particular find their application as intermediates in the production of fragrances,<sup>5</sup> pharmaceuticals,<sup>6</sup> detergents,<sup>7</sup> emulsifiers<sup>8</sup> and lubricants.<sup>9,10</sup> Common pathways used to produce fatty alcohols are (1) direct hydrogenation of oils and fats<sup>11,12</sup> or (2) hydrogenation of fatty acids and their methyl esters (FAME, biodiesel). The latter is a commodity chemical, produced annually on a 9 Mt scale in the European Union alone.<sup>13</sup> Many bulk chemicals including polyesters and polyurethanes<sup>14</sup> can be synthesised using diols<sup>14–17</sup> obtained *via* the hydrogenation of dicarboxylic acids and their esters.<sup>18–20</sup>

In a broader context, ester hydrogenation is also relevant as one of the key steps in a potential route to valorise carbon dioxide<sup>21,22</sup> and in green methanol production.<sup>23</sup> In the presence of homogeneous catalysts, CO<sub>2</sub> (or CO) can be reduced to methyl

<sup>a</sup> Inorganic Materials Chemistry group, Schuit Institute of Catalysis, Eindhoven University of Technology, P.O. Box 513, 5600 MB Eindhoven, The Netherlands.  
 E-mail: [e.a.pidko@tue.nl](mailto:e.a.pidko@tue.nl); Tel: +31-40-247-2189

<sup>b</sup> Institute for Complex Molecular Systems, Eindhoven University of Technology, P.O. Box 513, 5600 MB Eindhoven, The Netherlands

† Authors contributed equally.



James Pritchard

doctoral fellow in the group of Prof. Emiel J. M. Hensen and Dr Evgeny A. Pidko at Eindhoven University of Technology.

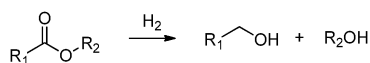
James Pritchard (Wales, UK, 1987) was educated at Cardiff University and received his PhD in 2013. He worked in the group of Prof. Graham J. Hutchings FRS at the Cardiff Catalysis Institute, developing noble metal catalysts for the direct synthesis of hydrogen peroxide. His research interests include the design and application of novel bimetallic catalysts for a range of hydrogenation and oxidation reactions. Since January 2014, he has been working as a post-



Georgy A. Filonenko

Georgy Filonenko (Elizovo, Russia, 1988) received his master degree in Chemistry from Novosibirsk State University in 2010 with Prof. Alexander Khassin. He is currently a PhD researcher under the supervision of Prof. Emiel J. M. Hensen and Dr Evgeny A. Pidko in the Inorganic Materials Chemistry group at Eindhoven University of Technology. His research is mainly focused on the mechanistic studies in catalytic hydrogenation reactions and synthetic organometallic chemistry.





**Scheme 1** General reaction for the hydrogenation of esters to alcohols

formate, which can then be further reduced at low temperature to methanol.<sup>24,25</sup>

Finally, the hydrogenation of carboxylic acid derivatives is a powerful tool in synthetic organic chemistry. Alcohol products typically formed in such reduction reactions offer great potential for further synthetic functionalization. For example, these alcohols can be derivatized by selective dehydrogenation,<sup>26,27</sup> oxidation,<sup>28,29</sup> amination<sup>30</sup> and acceptorless dehydrogenative coupling towards esters, amides and imines.<sup>31-33</sup> Consequently, the catalytic reduction of carboxylic acids and their esters can yield a vast number of useful products such as bulk platform chemicals or fine-synthesis intermediates.



Robbert van Putten

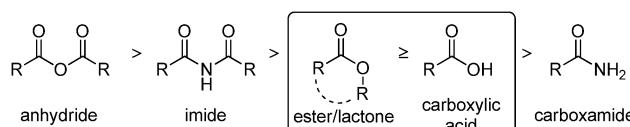
Volkan Degirmenci, he joined an MSc program at Eindhoven University in 2015.

Emiel J. M. Hensen

Institute on Catalysis (ERIC). His research interests include mechanisms of heterogeneous catalysis for natural and synthesis gas conversion, biomass conversion, as well as topics related to synthesis of porous catalysts and catalysis for solar fuels.

Historically, stoichiometric methods were used for the reduction of acids and esters. The Bouveault–Blanc-reduction<sup>34</sup> – one of the early methods used to reduce esters – involves reaction with elemental sodium in absolute ethanol.<sup>35</sup> In this process, a total of four equivalents of Na are required to convert the ester to the corresponding alcohol. Due to the risks associated with the handling of alkali metals and the significant production of waste, the Bouveault–Blanc reduction has largely been replaced by other processes involving metal-hydrides as reducing agents.<sup>36</sup> Such hydrides as  $\text{LiAlH}_4$  or  $\text{NaBH}_4$  can be successfully employed for the reduction of a wide range of esters. However, the stoichiometric nature of such processes results in large amounts of waste.<sup>20</sup> Other disadvantages include tedious work-up procedures and the hazards associated with the handling of highly reactive hydride compounds.<sup>37</sup> Compared to stoichiometric methods, catalytic processes are more attractive from environmental as well as economic viewpoints. They offer higher atom and energy efficiencies. In particular, the use of molecular  $\text{H}_2$  as the reducing agent allows reaching 100% atom efficiency.

Nevertheless, catalytic hydrogenation of carboxylic acids and their esters is a challenging transformation, particularly due to the low electrophilicity of the carbonyl carbon and the difficulties associated with polarizing the carbonyl group of the substrate.<sup>38</sup> Acid anhydrides are, accordingly, the most reactive towards reduction, followed by imides, esters, lactones, free acids and, finally, amides (Scheme 2). Additional complexity stems from the fact that esters, lactones and carboxylic acids may interconvert under applied reaction conditions. Given the



**Scheme 2** Comparison of the order of polarizability of the carbonyl group



Evgeny A. Pidko

Evgeny A. Pidko (Moscow, Russia, 1982) received his master degree in chemistry from the Higher College of Chemistry of the Russian Academy of Sciences in 2004 and earned his PhD from Eindhoven University of Technology in 2008. Since 2011 he holds an Assistant Professor position at the Department of Chemical Engineering and Chemistry and in the Institute for Complex Molecular Systems in Eindhoven. His research mainly focuses on mechanisms of catalytic reaction with a particular emphasis on catalysis for renewables. His work aims at formulation of design rules for new and improved catalytic systems through a complementary use of chemical theory and experiments.

different reactivities of acids, esters and lactones towards hydrogenation, the product distribution in the catalytic reaction may differ dramatically depending on the extent of interconversion.

As a result of the resistance of carboxylic acids, esters and lactones towards reduction, an effective catalyst formulation is required. Current heterogeneously-catalysed processes are operated at harsh conditions with temperatures in the range 200–300 °C and H<sub>2</sub> pressures of 140–300 bar.<sup>39</sup> Therefore, side reactions and degradation of the reaction substrates and products may occur. Although this might not be a concern for the production of many bulk or technical grade chemicals, it limits the applicability of this approach for the transformations of highly functionalized compounds in fine chemical synthesis. Even the reduction of relatively simple dicarboxylic acids and their esters can suffer from the formation of ethers, lactones, hydroxycarboxylic acids and hydrocarbons as by-products.<sup>40,41</sup>

Although conventional Cu and Zn chromite catalysts and RANEY® Ni can catalyse the reduction of esters and fatty acids<sup>42,43</sup> and they can even be chemoselective,<sup>43</sup> considerable improvements in catalyst performance are needed to improve the process in terms of economic efficiency and environmental impact. In addition, the harsh operation conditions needed to maintain the high activity of these catalysts may lower selectivity in the reduction of highly functionalised or less stable substrates. Therefore, the development of catalysts that display high chemoselectivity at reduced temperatures and pressures is desired. With these objectives, the search for new catalyst formulations has dominated the heterogeneous catalysis research field, with the majority of works featuring bimetallic catalyst design. Interestingly, heterogeneous catalysts developed during the last decade share many common properties with their homogeneous counterparts. For instance, they rely strongly on the cooperation between different catalyst components and show a pronounced bifunctional behaviour.

Regarding the growing interest and important findings reported in literature in recent years, heterogeneous catalysis will hold the main focus of this review. The most important developments in heterogeneous catalysis for conversion of carboxylic acid derivatives will be described. In addition, we will describe the recent advances in the field of homogeneous ester hydrogenation and discuss the similarities between homogeneous and heterogeneous hydrogenation catalysts. Until now, this comparison has been rarely made in the literature; we expect that drawing this parallel will prove useful for future research. Finally, we will present an outlook in which the reaction mechanisms proposed for heterogeneous and homogeneous catalysis will be assessed in an attempt to make a next step towards a unified mechanistic description of these catalytic systems.

## 2. Heterogeneous catalysis in ester hydrogenation

### 2.1 Early catalyst designs

Starting in the early 1930's, a series of important breakthroughs was made regarding the design and application of ester

hydrogenation catalysts. Pioneering works by Adkins focused on Cu/Cr/Ba oxide-containing catalysts and their application to a range of oxygenated substrates. Esters could be converted over these catalysts with the alcohol yields generally in excess of 90%.<sup>44–47</sup> Although Adkins-type catalysts (CuO/CuCr<sub>2</sub>O<sub>4</sub>) require harsh operating conditions, they are still used to manufacture fatty alcohols at the industrial scale due to resistance of the catalyst structure to free fatty acids. The composition of these catalysts has remained largely unchanged since their discovery.<sup>48–50</sup>

Due to the broad application of chromite-based catalysts, research into Cr-free alternative formulations has been undertaken and the use of Cu–Fe–Al mixed oxide systems was proposed.<sup>51</sup> It was found that the Cr-induced promotional effect on Cu was largely preserved on substituting the Cr component for Fe. Addition of Al was suggested to improve the catalyst stability by preserving the crystallinity of the Cu–Fe spinel (CuFe<sub>2</sub>O<sub>4</sub>) as well as a high dispersion of the active Cu phase. The comparable high activity, selectivity and stability of this catalyst were demonstrated during 20 days on-stream in a pilot plant facility with a capacity of 35 000 tpa.<sup>51</sup> In addition, the use of RANEY® Cu and Ni catalysts for the selective hydrogenation of carboxylic acids and their esters has also been reported in the patent literature.<sup>52–55</sup>

Studies on supported Cu catalysts have received much attention, with early works dealing with vapour-phase hydrogenation of simple esters such as methyl and ethyl acetate.<sup>56–59</sup> These studies on the model compounds provided a thorough insight into the kinetics of ester hydrogenation, which is well described in several articles by Evans *et al.* from the late-1980's.<sup>56–58</sup> Noteworthy, the hydrogenation of ethyl acetate over RANEY® Cu showed first order in H<sub>2</sub> and a –0.5 order in ethyl acetate.<sup>56</sup> In other works from this period, the rates of hydrogenation for a series of different esters containing the same acyl group were compared.<sup>57,58</sup> Studies addressing the hydrogenation of dimethyl succinate over copper chromite have also provided information on previously unknown reaction pathways.<sup>59</sup> The consecutive mechanism was highlighted in which the initial hydrogenation of dimethyl succinate to  $\gamma$ -butyrolactone (GBL) and CH<sub>3</sub>OH were followed by further hydrogenation of GBL to give THF and H<sub>2</sub>O. The low reactivity of Cr-free Cu/SiO<sub>2</sub> catalysts can be enhanced by the addition of ZnO.<sup>60–62</sup> Some controversy remains as to which Cu oxidation state(s) promote the reaction with some researchers claiming a high Cu<sup>0</sup> surface area favouring methanol synthesis,<sup>63</sup> while other experimental work implies that well-dispersed Cu<sup>+</sup> ions in close contact with ZnO phases may represent the catalytically active species.<sup>64</sup>

The long term stability of the catalyst is essential for industrial application. Critically, the hydrogenation of natural fatty acid esters over Cu-containing catalysts suffers from fast catalyst deactivation by sulphur and phosphate containing compounds present in bio-derived feedstocks.<sup>65–67</sup> This phenomenon has been thoroughly investigated for Cu/SiO<sub>2</sub> and Cu/ZnO/SiO<sub>2</sub>.<sup>65</sup> The ZnO-promoted catalyst deactivated *ca.* twice as fast as Cu/SiO<sub>2</sub> due to the high stability of the ZnS phase formed upon the decomposition of the sulphur-containing



poison molecules. Other studies<sup>66,67</sup> speculated that the degree of poisoning in the presence of alkylthiols and alkyl disulphide compounds is affected by alkyl chain length and sulphur concentration. It was proposed that catalyst deactivation may be due to such factors as the loss of Cu/Zn synergy as well as the reduction in both surface area and the pore volume. These studies pointed to the importance of such factors as the purity of fatty acid ester feedstock, tolerance of catalyst formulations to various feed impurities and the feasibility of applying catalyst regeneration steps to restore the catalytic performance in practical applications.

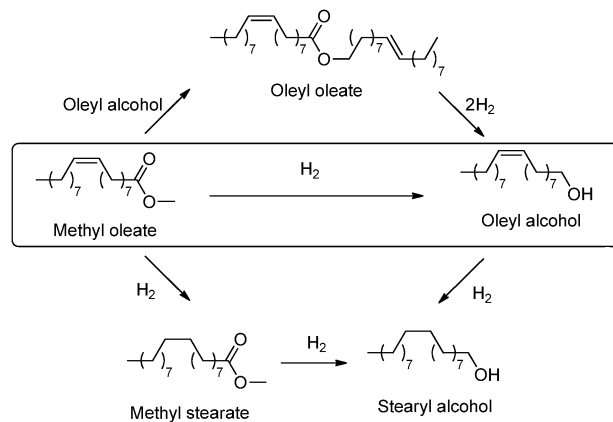
The performance of ZnO containing catalyst was further studied by the group of Barrault that showed that ZnO alone can activate both the carbonyl group of the ester molecule and dihydrogen.<sup>68</sup> However, ZnO-supported catalysts were also susceptible to fast deactivation in the presence of organic chlorides.<sup>69</sup> Specifically, for the hydrogenation of methyl laurate to lauryl alcohol using a Cu/ZnO catalyst, both conversion and selectivity towards lauryl alcohol selectivity decreased when the chloride concentration in the feed was increased from 0 to 0.5 mmol per gram of catalyst. Characterisation of the spent catalysts indicated a substantial Zn leaching together with the decrease of the surface area and metal particles sintering. Finally, the performance of Cu/ZnO catalysts in the hydrogenation of methyl laurate can also be impeded in the presence of water.<sup>70</sup> The occlusion of active sites, crystallite size growth, and the agglomeration of Cu/Zn particles were proposed to be responsible for deactivation.

Further insight into ZnO-supported catalysts was made by Gustafson *et al.*<sup>71</sup> who addressed the catalytic activity of Pd-Zn catalysts for hydrogenation of methyl acetate. It was shown that the rate of ester hydrogenation can be controlled by varying the Zn to Pd ratio in the catalyst. In particular, the rate of methyl acetate conversion by Pd-Zn (1:2) catalyst is four times higher than that of the Pd-Zn (1:1) formulation. However, the introduction of Zn also strongly promoted the transesterification between methyl acetate and ethanol product. This resulted in a decrease in ethanol selectivity from 63 to 46% on raising the Zn to Pd ratio from 1 to 2. Unfortunately, high temperatures and pressures (300 °C, 50 bar H<sub>2</sub>) were still required for the performance of Pd-Zn catalyst formulation.

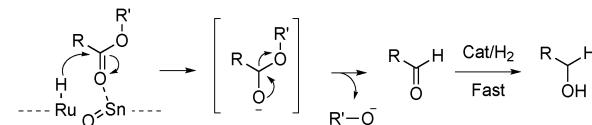
## 2.2 Sn and Ge-doped bimetallic catalysts

Despite their utility in chemoselective FAME hydrogenation,<sup>72</sup> Cu-based catalysts display low activity and require harsh reaction conditions. Therefore, the development of alternative catalysts that can operate at milder conditions is essential. Significant progress in this direction has been associated with supported bimetallic catalysts. The activity of these systems stems from the bifunctional nature of catalysis originating when the Lewis-acid promoter(s) are located in close proximity to a transition metal centre. First examples of such catalysts utilized Sn as a promoter for Ru-catalysed hydrogenation of carboxylic acids and their esters.

Seminal studies by the group of Narasimhan<sup>73,74</sup> demonstrated that methyl oleate could be selectively hydrogenated to



Scheme 3 Reaction scheme of the hydrogenation of methyl oleate to oleyl alcohol.<sup>73,74</sup>



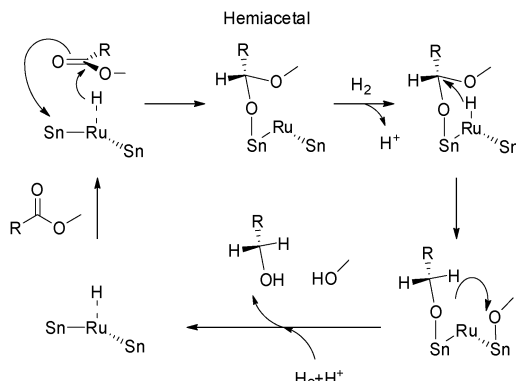
Scheme 4 A simplified mechanism proposed for the hydrogenation of esters using Ru-Sn-B supported catalysts.<sup>74</sup>

oleyl alcohol (Scheme 3) in the presence of the NaBH<sub>4</sub>-reduced Ru-Sn-B/Al<sub>2</sub>O<sub>3</sub> (Ru/Sn = 1:2) catalyst at 270 °C and 44 bar H<sub>2</sub> pressure. Under these conditions, 80% methyl oleate conversion with 62% selectivity towards oleyl alcohol were obtained within 7 hours. Detailed characterization of the catalyst indicated the importance of an intimate contact between boron and the catalytically active Ru phase. It was suggested that the role of the B promoter was to enhance the electron density of surface Ru species, while the presence of Sn favoured a high dispersion of metallic Ru. X-ray Photoelectron Spectroscopy (XPS) evidenced the presence of Sn<sup>2+</sup> and Sn<sup>4+</sup> species as well as the separate alloyed Ru<sub>3</sub>Sn<sub>7</sub> phase in the final catalyst. Therefore, in a proposed reaction mechanism, metallic Ru sites promote the H<sub>2</sub> dissociation while the adjacent Sn<sup>2+</sup>/Sn<sup>4+</sup> Lewis acid sites polarize the carbonyl group of methyl oleate. The latter facilitates the hydride transfer from the adjacent Ru-H sites to form an anionic species. This species can then be rapidly hydrogenated towards the alcohol *via* the intermediate formation of a reactive aldehyde molecule (Scheme 4). Simultaneously, the OR' moiety adjacent to the carbonyl group is eliminated and converted to an alcohol. The role of the Ru<sub>3</sub>Sn<sub>7</sub> phase in this reaction was assumed to be negligible.

Further analysis of Ru-Sn cooperativity and the role of the catalyst support was performed by Barrault and co-workers.<sup>75</sup> Their data pointed to the involvement of mixed Ru-Sn sites in the hydrogenation reaction that proceeds *via* a hemiacetal intermediate (Scheme 5).

Rios and co-workers<sup>76</sup> compared the influence of different Ru and Sn precursors on the preparation of Ru-Sn/Al<sub>2</sub>O<sub>3</sub> catalysts and their performance in methyl oleate hydrogenation. Similar to ZnO supported catalysts, a strong negative





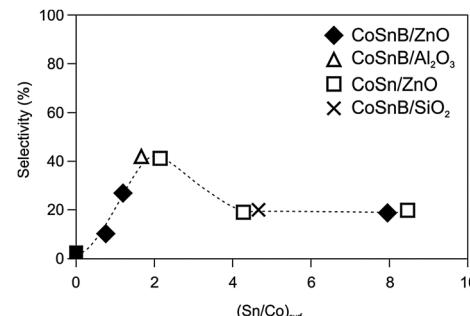
**Scheme 5** Proposed mechanism for the direct hydrogenation of methyl oleate into unsaturated alcohol over an  $\text{Ru-Sn}/\text{Al}_2\text{O}_3$  catalyst.<sup>75</sup>

effect of chlorides on the activity of Ru-Sn catalysts was observed. Therefore catalyst calcination/reduction cycles are required to minimise the chloride content in the final material if Cl-containing Ru and Sn precursors are utilized. Alternatively, chlorine-free precursors could be used. The most active Ru-Sn catalyst was obtained by reducing  $\text{RuCl}_3$  and  $\text{SnCl}_2$  precursors in the presence  $\text{NaBH}_4$ . With such a catalyst methyl oleate conversion of 75% with identical selectivity towards oleyl alcohol was reached at 270 °C. More detailed analysis of the chloride effect suggested that residual Cl species may affect the metal dispersion in the final catalyst.

Alongside Ru-Sn systems, other Sn-containing catalysts include Rh-Sn that was recently investigated for the hydrogenation of neat methyl laurate ( $\text{C}_{13}\text{H}_{26}\text{O}_2$ ) and methyl palmitate ( $\text{C}_{17}\text{H}_{34}\text{O}_2$ ) esters.<sup>77</sup> Unfortunately, the formation of transesterification products in the absence of catalyst and at temperatures above 200 °C was observed. However, this effect could be reversed to some extent by employing catalysts capable of hydrogenating the transesterification products. Comparison of several other transition metals indicated that bimetallic Ru-Co, Ru-Zn, Co-Zn and Ru-Cu catalysts could not be efficiently used for FAME hydrogenation due to the preferential formation of lauric acid over the desired hydrogenation to lauryl alcohol.

Further research on Sn-promoted catalysts was conducted by the group of Barrault.<sup>68,75,78-80</sup> The authors confirmed the advantage of the Sn-rich Sn-Ru catalyst formulations, and importantly, demonstrated the possibility of substituting the noble metal Ru component by cobalt. All Co-Sn/ZnO catalysts studied by Barrault and co-workers<sup>75</sup> provided moderate conversions of methyl oleate with alcohol selectivities reaching *ca.* 50% (Scheme 6). Similar to their noble-metal containing counterparts, the active Co-Sn formulations showed a strong interaction between the catalyst components. The cooperative action of the metallic Co and oxidic Sn species represented in the simple form as  $[\text{Co}^0\ldots(\text{SnO}_x)_2]$  was proposed to determine the activity of the respective catalyst in ester hydrogenation.

The authors proposed that the Co-Sn interactions are weaker than metal-support interactions<sup>78</sup> and, therefore, the preparation method to obtain Co-Sn catalysts markedly



**Scheme 6** Comparison of oleyl alcohol selectivity over different Co-Sn catalysts and as a function of  $\text{Sn/Co}$  surface atomic ratio. Reaction conditions: stainless steel batch reactor (300 mL), methyl oleate (neat, 100 mL), catalyst (2.2 g), 270 °C, 80 bar  $\text{H}_2$ .<sup>75</sup>

influences catalytic performance. Catalysts reduced by  $\text{NaBH}_4$  (CoSnB) were significantly more active than their counterparts prepared by sol-gel or dry impregnation methods. It was concluded that the treatment with  $\text{NaBH}_4$  led to a deeper reduction of both Co and Sn catalyst components.

Finally, Ge – another 14 group element, can be used instead of a Sn promoter. Bimetallic 1%<sub>wt</sub> Ru- $x\%$ <sub>wt</sub> Ge-B/Al<sub>2</sub>O<sub>3</sub> ( $x = 1-4$ ) catalysts are capable of hydrogenating methyl oleate with conversions up to 80%.<sup>81</sup> However, the yields of oleyl alcohol were low (*ca.* 20%) due to the competitive hydrogenation of the C=C bond resulting in methyl stearate or stearyl alcohol (Scheme 3). The optimal selectivity to oleyl alcohol was obtained with a Ru:Ge weight ratio of 1:2. Surprisingly, deviation towards Ru:Ge ratios of 1:1 and 1:3 effectively suppressed formation of oleyl alcohol. In all cases, hydrogenation of the C=C bond could not be adequately suppressed and was likely promoted by Ge species covering active surface Ru sites as is suggested by significant broadening in the particle size distribution when moving from monometallic Ru-B (comprising *ca.* 2 nm particles) to the bimetallic Ru-Ge-B/Al<sub>2</sub>O<sub>3</sub> catalyst composition (Fig. 1).

### 2.3 Catalyst support and solvent effects in ester hydrogenation

Cooperative sites alternative to those provided by group 14 promoters (Sn and Ge) can be located on the catalyst support. Initially, the role of the support surface hydroxyl groups and solvent effects was studied by Li and co-workers for another bimetallic catalyst – Ru-Pt/AlOOH.<sup>82</sup> Prepared by the co-impregnation of Ru and Pt metals onto  $\gamma\text{-Al}_2\text{O}_3$  and subsequent hydrothermal treatment converting the support to the boehmite, the resulting catalyst was found to be highly effective at hydrogenating methyl propionate in aqueous environments. Here, the interaction of the substrate with the surface hydroxyl groups as well as water *via* hydrogen bonding was proposed to promote ester hydrogenation. Under significantly improved conditions (180 °C, 50 bar  $\text{H}_2$ ) the catalyst provided methyl propionate conversion up to 90% with 98% selectivity for 1-propanol.

Further insight into the participation of solvent and catalyst support in ester reduction was reported by the same group of



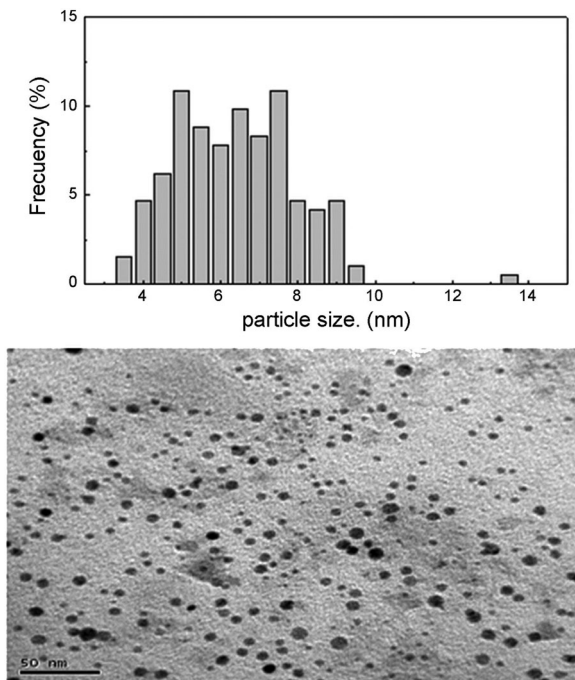
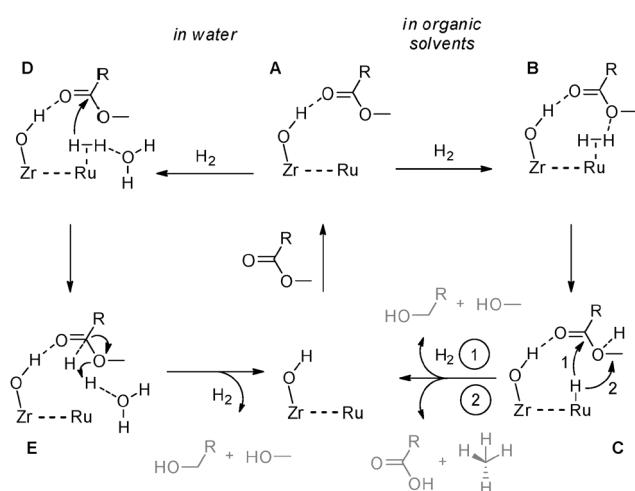


Fig. 1 TEM and particle size distribution measurements for 1% Ru-1% Ge-B/Al<sub>2</sub>O<sub>3</sub>. Reproduced from Sánchez *et al.* *Catal. Today*, 2013, **213**, 81–86.<sup>81</sup> by permission of Elsevier.



Scheme 7 Reaction mechanism of the hydrogenation of methyl propionate over an Ru/ZrO<sub>2</sub>·xH<sub>2</sub>O catalyst in water or organic solvents.<sup>83</sup>

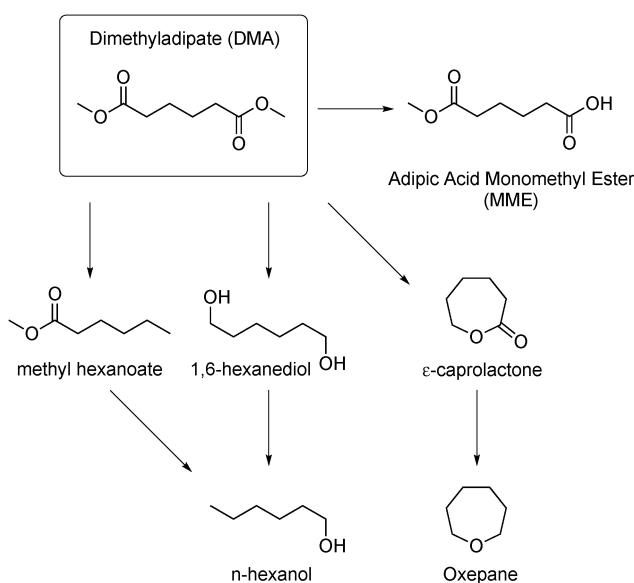
researchers<sup>83</sup> using a 7.9%<sub>wt</sub> Ru/ZrO<sub>2</sub>·xH<sub>2</sub>O catalyst (Scheme 7). Similar to their previous work, Li and co-workers highlighted the role of water as a proton acceptor facilitating the heterolytic H<sub>2</sub> cleavage. As a result, a reaction mechanism emphasizing the synergy between the Zr-bound hydroxyl groups, Ru centres and water solvent has been proposed. The hydrogen bonding of the substrate with surface hydroxyl groups (A, Scheme 7) polarizes the carbonyl moiety and facilitates the difficult hydride insertion step (C). The mechanism of H<sub>2</sub> activation was proposed to depend on the solvent employed. In water, H<sub>2</sub>O molecules act as base mediators (D) that transfer H<sup>+</sup> formed upon the heterolytic

cleavage of H<sub>2</sub> to the pre-coordinated substrate molecules (E). Therefore, the subsequent hydrogenation of the substrate molecule is facilitated. When the reaction is carried out in organic solvent, the ester functionality itself plays the role of the base in the heterolytic H<sub>2</sub> cleavage (B), making the overall process less efficient. These considerations were supported by the experimental observations on the strong promoting effect of the water solvent compared to hexane and different short-chain alcohols and diol solvents. In aqueous medium the yields of 1-propanol were close to 95% at temperatures as low as 150 °C.

Carvalho and co-workers<sup>84</sup> have also evaluated a series of related catalysts based on aluminium pillared clays, denoted as Al-PILC, for the hydrogenation of diesters such as dimethyl adipate. Even in the absence of Ru and Sn metals, these catalysts afforded up to 95% ester conversion, although with no selectivity for diol product. This activity was attributed to a high concentration of surface acid sites (3 per nm<sup>2</sup>) within the clay structure. The hydrogenation of diesters can in theory yield a wide range of products since either one or both carbonyl groups may be converted to acid, alcohol and alkane. Scheme 8 summarizes the possible reactions products for methyl adipate hydrogenation.

The formation of other products apart from 1,6-hexanediol over Al-PILC supported Ru catalysts could be reduced by roughly 50% upon the addition of barium that is believed to reduce the clay acidity.

The addition of Sn to Ru was beneficial in terms of conversion and selectivity to commercially important cyclic products, such as  $\epsilon$ -caprolactone, methyl caproate and caproic acid. Dimethyl adipate hydrogenation was also examined in the presence of Ru-Sn catalysts on different supports by the group of Fraga.<sup>85</sup> It was suggested that Sn enhances the formation of 1,6-hexanediol for bimetallic 2%<sub>wt</sub> Ru-4.7%<sub>wt</sub> Sn (Ru/Sn = 1:2 molar) catalysts. No diol formation was observed using monometallic Ru catalysts,



Scheme 8 Summary of the possible products derived from the hydrogenation of dimethyl adipate.<sup>84</sup>

suggesting Ru–Sn cooperativity to be crucial for the diol formation. Furthermore, the type of the support was also found to influence the diol selectivity. In the series  $\text{TiO}_2 > \text{CeO}_2 > \text{SiO}_2 > \text{Nb}_2\text{O}_5 > \text{Al}_2\text{O}_3$ , the selectivity dropped from 29% to 6% in a 10 h experiment at 255 °C under 50 bar  $\text{H}_2$ .

Other studies<sup>86–89</sup> have suggested that the relative concentrations of metallic and ionic Sn species can be controlled by the type of the support material used in the catalyst. In particular, metallic Sn species are found to be favoured on acidic and amphoteric supports such as carbon and  $\text{TiO}_2$ ,<sup>86,87</sup> while cationic  $\text{Sn}^{2+}/\text{Sn}^{4+}$  species are predominantly formed on basic oxides such as  $\text{Al}_2\text{O}_3$  and  $\text{MgO}$ .<sup>75,88</sup> It is important to note that on  $\text{Al}_2\text{O}_3$ , the existence of both metallic and ionic Sn species has been acknowledged.<sup>73,75</sup>

#### 2.4 Coinage metal-based catalysts for hydrogenation of FAMEs and diesters

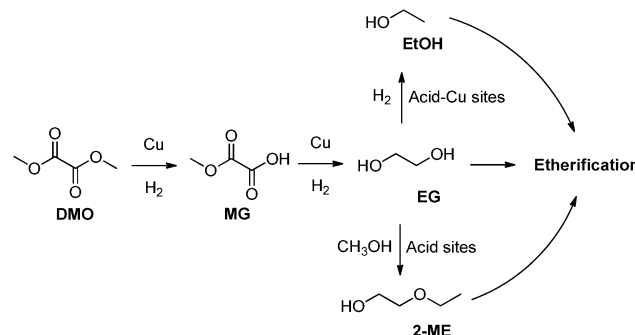
Finally, coinage metals (Cu, Ag, Au) can act as promoters to platinum group metals or comprise potent FAME hydrogenation catalysts on their own. For example, bimetallic Pd–M (M = Cu, Co, Ni) catalysts supported on diatomite show the highest catalytic activity when Pd is promoted by Cu.<sup>90</sup> A 1%<sub>wt</sub> Pd–Cu (3:1)/diatomite catalyst tested in hydrogenation of methyl palmitate, stearate and laurate was very active and allowed a methyl palmitate conversion of 98% with 84% selectivity to 1-hexadecanol (Table 1). The transesterification product, palmityl palmitate, was also formed along with *n*-hexadecane resulting from the dehydration of 1-hexadecanol. The former reaction becomes dominant at elevated temperatures where a substantial decrease in the yield of 1-hexadecanol was observed.

Extensive attention in the literature has been paid to the use of Cu-based catalysts for the hydrogenation of diesters, for example, dimethyl oxalate (DMO, Scheme 9) to ethylene glycol (EG).<sup>14,15,17,91–99</sup> For Cu–HMS (hexagonal mesoporous silica) catalysts, activity depended on the Cu loading, textural and structural properties.<sup>91</sup> Complete dimethyl oxalate conversion and greater than 90% selectivity to ethylene glycol could be achieved using 5%<sub>wt</sub> Cu/HMS under optimized conditions (200 °C, 25 bar  $\text{H}_2$ ). Catalyst characterization revealed small Cu particles and more than one Cu oxidation state in the final catalyst, thereby making it difficult to deduce the active species

Table 1 Effect of reaction temperature on the activity of 1% Pd–Cu (3:1)/diatomite catalyst for methyl palmitate hydrogenation<sup>a</sup>

Entry	$T$ (°C)	Conv. (%)	Selectivity (%)		
			$n\text{-C}_{16}\text{H}_{33}\text{OH}$	Other	Y (%) of $n\text{-C}_{16}\text{H}_{33}\text{OH}$
1	250	67.5	85.9	14.1	57.9
2	260	93.3	84.6	15.4	78.9
3	270	98.8	83.9	16.1	82.9
4	280	99.8	50.9	49.1	50.8
5	290	99.9	24.5	75.5	24.5
6	300	99.9	21.9	78.1	21.9

<sup>a</sup> Conditions: catalyst (20 mg), substrate (0.1 g), solvent (*n*-heptane, 1 mL), 55 bar  $\text{H}_2$ , 7 h.<sup>90</sup>



Scheme 9 Reaction pathways for the conversion of DMO over copper catalysts under hydrogenation reaction conditions.<sup>99</sup>

Table 2 Summary of physicochemical properties of as-synthesized Cu–HMS catalysts

Catalyst	Cu (% <sub>wt</sub> )	$S_{\text{BET}}$ (m <sup>2</sup> g <sup>-1</sup> )	$S_{\text{Cu}}^a$ (m <sup>2</sup> g <sup>-1</sup> )	$d_{\text{pore}}$ (nm)	$V_{\text{pore}}$ (cm <sup>3</sup> )	$d_{\text{Cu}}^b$ (nm)
HMS	—	970	—	4.2	0.90	—
IE-CuNH	19.5	239	9.3	7.2	0.57	5.0
IE-CuCl	13.4	595	1.3	3.0	0.55	31.6
IE-CuAC	16.3	111	3.2	11.2	0.37	5.2
IE-CuCO	16.6	224	7.8	7.8	0.56	5.1

<sup>a</sup> Determined by  $\text{N}_2\text{O}$  titration. <sup>b</sup> Calculated using Scherrer equation.<sup>93</sup>

for this reaction.<sup>17,92</sup> The effect of Cu source was also studied for  $\text{Cu}(\text{acac})_2$ ,  $\text{CuCl}$ ,  $\text{Cu}(\text{OH})_2\text{CO}_3$  and  $\text{Cu}(\text{NH}_3)_4(\text{NO}_3)_2$  precursors.<sup>93</sup> The highest ethylene glycol yield of 98% was achieved by using  $\text{Cu}(\text{NH}_3)_4(\text{NO}_3)_2$ . This was attributed to the high concentration and dispersion of active Cu sites, which was determined by the degree of the initial interaction between Cu precursor ions and the support (Table 2).

The interest in the utilization of Cu species supported on materials of high surface area and porosity has also been expressed by Yuan and co-workers<sup>94</sup> in their studies evaluating the performance of Cu/SiO<sub>2</sub> hybrid catalysts containing the H-ZSM-5 zeolite. The addition of 3%<sub>wt</sub> H-ZSM-5 to Cu/SiO<sub>2</sub> increased the conversion of dimethyl oxalate to 99.5% and selectivity to ethylene glycol to 94.8%. This was achieved by the precise modification of growth parameters associated with the cupric phyllosilicate phase,  $\text{Cu}_2\text{Si}_2\text{O}_5(\text{OH})_2$ ,<sup>14,94</sup> which resulted in improved surface area, concentration and dispersion of Cu<sup>+</sup> species. The increased acidity and hydrogen absorption capacity<sup>100</sup> of H-ZSM-5 may also account for the enhanced activity shown by the hybrid catalysts. Noteworthy, product distribution varied considerably depending on the acidic properties of the support. Whereas the high selectivity to ethylene glycol was reached with Cu/SiO<sub>2</sub>, the etherification product, 2-methoxyethanol (2-ME, Scheme 9), was the main product formed over Cu/Al<sub>2</sub>O<sub>3</sub> catalysts.<sup>99</sup> However, simply changing the solvent from methanol to 1,4-dioxane could minimise the formation of 2-ME and simultaneously increase the yield of ethanol to 95.5% by suppressing efficiently the etherification path.

Some improvement in the DMO hydrogenation activity was associated with further optimization of the Cu/SiO<sub>2</sub> catalyst preparation procedure. The ammonia-evaporation method<sup>96</sup>

**Table 3** Production of ethylene glycol (EG) and methyl glycolate (MG) by dimethyl oxalate hydrogenation by Au–Ag catalysts at different temperatures<sup>a</sup>

Catalyst (Au% <sub>wt</sub> ): (Ag% <sub>wt</sub> )/SBA-15	T (°C)	Conv. (%)	Selectivity (%)	
			MG	EG
8:0	145	3.4	99.9	0.1
	235	65.9	99.9	0.1
8:0.5	145	78.4	99.9	0.1
	235	99.9	68.4	31.6
8:0.75	145	97.2	98.9	1.1
	235	99.9	66.3	33.7
8:1.5	145	99.5	94.2	5.8
	235	99.8	10.4	89.6
8:4.5	145	0.2	99.5	0.5
	235	99.9	1.7	98.3
0:4.5	145	0.4	99.9	0.1
	235	99.9	95.6	4.4

<sup>a</sup> Reaction conditions: WLHSVDMO = 0.6 h<sup>-1</sup>, 30 bar H<sub>2</sub>, H<sub>2</sub>/DMO molar ratio = 100.<sup>98</sup> MG = methyl glycolate, EG = ethylene glycol.<sup>97</sup>

for Cu deposition onto SiO<sub>2</sub>, and a post-synthetic impregnation with boric acid<sup>97</sup> both yielded active and selective catalysts. Cooperation between Cu<sup>0</sup> and Cu<sup>+</sup> states was proposed to define the catalytic activity, while the boric acid was proposed to regulate the Cu<sup>0</sup>/Cu<sup>+</sup> content through the strong interactions between the acidic boric oxide and Cu species.

Dialkyl oxalates are also readily hydrogenated at reduced temperatures and pressures over supported bimetallic Au–Ag and Au–Cu catalysts.<sup>97,98</sup> A dramatic improvement of dimethyl oxalate conversion in Au-catalysed hydrogenation was observed upon introduction of Ag into the SBA-15-supported catalyst (Table 3).<sup>97</sup>

Addition of small amounts of Ag to Au/SBA-15 resulted in almost full conversion of DMO, even at temperatures as low as 145 °C. The product distribution (methyl glycolate vs. ethylene glycol) depended on reaction temperature and relative catalyst composition. For several bimetallic Au–Ag catalysts, the major product at 145 °C was methyl glycolate while ethylene glycol was mainly formed at 235 °C. A nearly 100% selectivity was obtained with 8%<sub>wt</sub> Au–4.5%<sub>wt</sub> Ag/SBA-15. Authors suggested the importance of the concerted action of the Au–Ag pair. Namely, the interaction with H<sub>2</sub> is facilitated by silver<sup>101</sup> while Au has a strong affinity for the carbonyl group.<sup>102</sup> The resulting cooperative action of this catalyst is therefore similar to that of Ru–Sn<sup>74</sup> and Pt–Re<sup>103</sup> systems.

### 3. Bifunctional heterogeneous catalysis for the hydrogenation of carboxylic acids

Hydrogenation of free carboxylic acids to alcohols also represents an industrially important reaction. Selectivity in this reaction depends on the type of catalyst used and apart from alcohol products, alkanes and CO<sub>2</sub> can be produced via decarboxylation.<sup>104</sup> Similar to ester hydrogenation, common acid hydrogenation catalysts are bifunctional and exploit

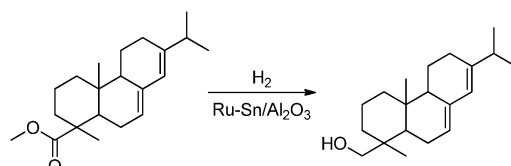
metal–metal, metal–support or more complex ensembles of bimetallic pair and catalyst support cooperations altogether.

An extensive study of a series of transition metal catalysts containing group 6–10 elements was carried out by Fuchikami and co-workers in 1995.<sup>105</sup> Authors reported a near negligible performance of monometallic catalysts in the hydrogenation of pentadecanoic acid at 180 °C and 100 bar H<sub>2</sub> pressure. Interestingly, they achieved extremely high alcohol yields using bimetallic catalysts comprising early transition metal carbonyl complexes in contact with a late metal complex at substantially lower temperatures (140–160 °C). Prime examples included Ru(acac)<sub>2</sub> or Rh/Al<sub>2</sub>O<sub>3</sub> in combination with Re<sub>2</sub>(CO)<sub>10</sub> or Mo(CO)<sub>6</sub> precursors, all of which gave pentadecanol yields in excess of 90%. These bimetallic catalysts were shown to preferentially hydrogenate the carboxylic acid function in the presence of esters. Namely, a monomethyl ester of  $\alpha$ ,  $\omega$ -pentadecane dicarboxylic acid was hydrogenated to  $\omega$ -hydroxy ester in yields over 80%. This work laid the foundation for the development of various bifunctional catalysts for carboxylic acid hydrogenation. In fact, the majority of bimetallic combinations discovered by Fuchikami were further studied in detail by a number of researchers.

#### 3.1 Ruthenium-based catalysts

A significant shift towards lower reaction temperatures in Ru-catalysed acid hydrogenation was reported by Gallezot and co-workers.<sup>106</sup> Their work addressed the hydrogenation of arabinic acid, which can be produced by oxidative decarboxylation of glucose. At temperatures as low as 80–100 °C, Ru/TiO<sub>2</sub> and Ru/C catalysts could provide nearly full conversions of the acid under 100 bar H<sub>2</sub> pressure. However, the most active 5.1%<sub>wt</sub> Ru/C catalyst required a sodium anthraquinone-2-sulfonate promoter to achieve the best selectivity towards arabinol (*ca.* 99%). The promoter was shown to bind to the catalyst support permanently, thus allowing for the catalyst recycling.

In 1996, Tahara compared the effect of several non-toxic Sn precursors<sup>107</sup> for the hydrogenation of rosin to rosin alcohol at 260 °C using bimetallic Ru–Sn/Al<sub>2</sub>O<sub>3</sub> catalysts prepared by impregnation (Scheme 10). The yield of rosin alcohol decreased in the order: K<sub>2</sub>SnO (84%) > Na<sub>2</sub>SnO (77%) > tin 2-ethylhexanoate (68%) > SnCl<sub>2</sub> (22%). Residual K or Na originating from K<sub>2</sub>SnO and Na<sub>2</sub>SnO precursors was experimentally detected in the resulting catalysts. The presence of alkali metals was proposed to promote the C=O hydrogenation activity. It was later established<sup>108</sup> that calcination of Sn/Al<sub>2</sub>O<sub>3</sub> at 650 °C followed by addition of Ru and subsequent reduction at 450 °C provided the most active catalyst. This catalyst was used in the



**Scheme 10** Hydrogenation of abietic acid methyl ester, a major constituent of rosin, to its corresponding alcohol.<sup>106</sup>



hydrogenation of a range of aliphatic and aromatic acids to their corresponding alcohols (yields in brackets), including hexanoic acid (86%), lauric acid (94%), 2-ethylhexanoic acid (67%), cyclohexane carboxylic acid (74%), oleic acid (76%) and benzoic acid (94%). These results show that such Ru–Sn catalyst can selectively hydrogenate the C=O bond without hydrogenating C=C and aromatic groups.

Toba *et al.*<sup>109</sup> compared the hydrogenation of a series of dicarboxylic acids using a 2%<sub>wt</sub> Ru–Sn/Al<sub>2</sub>O<sub>3</sub> catalyst at 250 °C and 65 bar H<sub>2</sub> pressure. Authors found that high conversion of isophthalic, succinic, suberic and phthalic acids was possible, although the product selectivity varied significantly. Very low diol yields were obtained with succinic and terephthalic acid substrates, while high diol yields in excess of 85% were achieved in the hydrogenation of adipic, suberic and azelaic acids. For succinic acid, the hydrogenation yielded only 10.4% 1,4-butanediol with major products being tetrahydrofuran (57.1%) and  $\gamma$ -butyrolactone (30.4%). The structure of the carboxylic acid was assumed to account for all of the by-products described above, since isophthalic (*meta*-) and terephthalic acid (*para*-) could not be converted into lactones, while the other isomer, phthalic acid (*ortho*-), could be hydrogenated to benzobutyrolactone in high yield (80.4%). Finally, diols were also favoured when the chain length of aliphatic acids was increased. This was explained in part by the difficulty of the ring closure to form lactones with large cycles. Hara *et al.*<sup>110</sup> studied the effect of addition of Pt metal to Ru–Sn/C catalysts used for the hydrogenation of 1,4-cyclohexanedicarboxylic acid (CHDA, Scheme 11) to cyclohexane dimethanol (CHDM). Authors found that the leaching of Sn metal from the bimetallic Ru–Sn catalysts in the presence of acids could be largely suppressed by the addition 2%<sub>wt</sub> Pt. Addition of Pt was also suggested to promote the reduction of Ru and promote Ru–Sn interactions. Alternatively, Pt could enhance the catalytic activity by promoting the reduction of Sn species. This ultimately led to increased selectivity to the CHDM product. However, harsh conditions (230 °C, 85 bar H<sub>2</sub>) were still

required to achieve a high CHDA conversion and obtain selectivity to CHDM greater than 80%.

The formation of Ru–Sn ensembles was also proposed by the group of Zhu,<sup>111</sup> who highlighted a relationship between the choice of Sn precursor and catalyst support for the hydrogenation of CHDA. Al<sub>2</sub>O<sub>3</sub> was the preferred support that enhanced the activity and provided CHDM yields close to 98%.

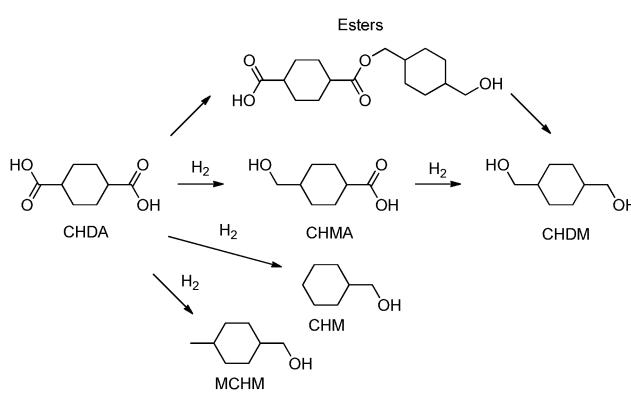
Chemoselective hydrogenation of acids using Ru–Sn catalysts was also realized. The oleic acid reduction to oleyl alcohol using a boron-doped Ru–Sn/Al<sub>2</sub>O<sub>3</sub> catalyst was studied by Pieck and co-workers.<sup>112</sup> Authors found that C=O hydrogenation proceeds with a higher activation energy than the competing C=C hydrogenation, which resulted in an optimal yields of oleyl alcohol achievable at higher temperatures.

The influence of preparation routes of Ru–Sn/Al<sub>2</sub>O<sub>3</sub> and TiO<sub>2</sub> catalysts on oleic acid hydrogenation activity was investigated by Mendes *et al.*<sup>113</sup> The sol–gel and conventional impregnation methods were compared. It was concluded that Ru–Sn/TiO<sub>2</sub> prepared by impregnation was more active and selective towards oleyl alcohol. Monometallic Ru counterparts were also found to be active for this reaction and favoured the production of stearly alcohol over oleyl alcohol. This therefore confirms previous suggestions that Sn suppresses the C=C bond hydrogenation path and promotes C=O hydrogenation by polarizing the carbonyl group *via* the interaction with the Lewis acidic Sn sites.

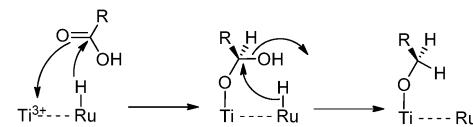
Since Ru/TiO<sub>2</sub> catalysts in particular were shown to be capable of hydrogenating the C=O bond in the absence of Sn promoter, the role of titania was discussed in detail and a reaction mechanism was proposed (Scheme 12).

Surface Ti<sup>3+</sup> defect sites were suggested to participate in the hydrogenation of the carbonyl group of the carboxylic acid. This reaction mechanism features the strong metal support interactions, with titania not only stabilizing highly dispersed Ru particles needed to facilitate hydrogenation but also playing a direct role in the reaction by polarizing the carbonyl group. Studies by Vannice and co-workers<sup>114</sup> also confirmed the oxide support involvement in the hydrogenation of acetic acid over supported Pt catalysts and render TiO<sub>2</sub> to be superior to SiO<sub>2</sub>, Al<sub>2</sub>O<sub>3</sub> and Fe<sub>2</sub>O<sub>3</sub> supports. The reaction was suggested to directly involve the interaction with the sites on the oxide surface.

Recently, Corma and co-workers<sup>115</sup> compared the activity of Ru nanoparticles supported on TiO<sub>2</sub> and carbon (0.64%<sub>wt</sub> Ru) in hydrogenation of lactic acid. Titania-supported catalysts were found to be three-fold more active compared to Ru/C. In addition to activation of the carbonyl group over TiO<sub>2</sub>, the activity was shown to be influenced by the metal loading and dispersion. In particular, the high activity of Ru/TiO<sub>2</sub> was

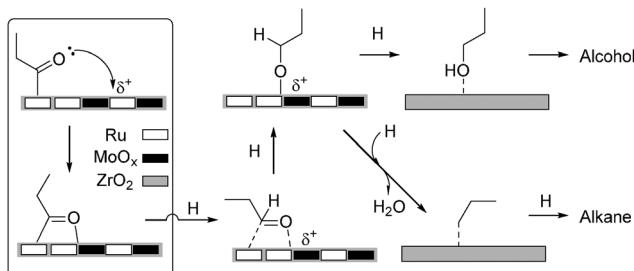


Scheme 11 The hydrogenation of 1,4-cyclohexanedicarboxylic acid (CHDA) to cyclohexanemethanol carboxylic acid (CHMA) and cyclohexane-dimethanol (CHDM), in addition to other possible hydrogenation products including esters, hydroxymethyl cyclohexane (CHM) and 1,4-hydroxymethyl cyclomethylhexane (MCHM), respectively.<sup>110</sup>



Scheme 12 Proposed mechanism for hydrogenation of carboxylic group over Ru/Ti catalysts.<sup>113</sup>





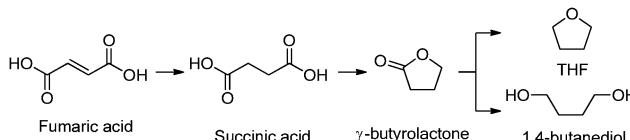
**Scheme 13** Surface reaction model for the hydrodeoxygenation of propanoic acid to propanol over Ru–Mo/ZrO<sub>2</sub> catalysts *via* formation of an  $\eta^2$ -(C,O) propanoyl intermediate species.<sup>116</sup>

attributed to the formation of small and highly dispersed Ru nanoparticles (*ca.* 2.0 nm) on TiO<sub>2</sub> and strong metal–support interactions. The resulting catalyst was shown to remain active in at least three successive reactions.

Ru-based catalysts can also be promoted by Mo oxide phases. Report by Zhu and co-workers<sup>116</sup> indicated synergy between the Ru and MoO<sub>x</sub> phases in 1%<sub>wt</sub> Ru–Mo/ZrO<sub>2</sub> catalysts active for the hydrogenation of propanoic acid. The interface between Ru and MoO<sub>x</sub> phases was proposed to stabilize the  $\eta^2$ -(C,O) propanoyl intermediate during the formation of propanol (Scheme 13). Later work<sup>117</sup> which assessed a wide range of supports for the Ru-catalysed aqueous phase reforming of propanoic acid also proposed identical metal–support bound intermediates.

Two pathways were proposed for the hydrogenation over Ru–Mo/ZrO<sub>2</sub>; one leading to methane, ethane and CO<sub>2</sub>, and the other to propanol and propane. The first pathway was proposed to take place over Ru-only particles, where the C–C bond adjacent to carbonyl group in propanoic acid is cleaved, yielding methane, ethane and CO<sub>2</sub>. The second mechanism is promoted by Ru–MoO<sub>x</sub> interface *via* the formation of an  $\eta^2$ -coordinated propanoyl intermediate where metallic Ru sites in close contact with MoO<sub>x</sub> species interact with the carbon and oxygen atoms of the carbonyl group, respectively. The existence of absorbed propanoyl species was evidenced by diffuse reflectance FTIR (DRIFTS) spectroscopy. The selectivity towards propanol under continuous flow conditions (190 °C, 64 bar H<sub>2</sub>) was increased by careful variation of the Ru/Mo atomic ratio and the best result was 64% selectivity at 58% conversion.

A similar mechanism was suggested for hydrogenation of propanoic acid over supported monometallic Ru catalysts.<sup>117,118</sup> Among the different supports studied, the adsorbed propionate and propanoyl species were found to be most stable on ZrO<sub>2</sub>. Furthermore, the presence of a high number of Lewis acid sites and strong metal support interactions after Ru addition was deemed crucial for selective C=O hydrogenation due to the formation of metal–acid surface sites.<sup>117</sup> This result suggests that the development of metal–acid cooperative sites is critical for limiting the C–C bond cleavage, which is more pronounced over Ru catalysts containing fewer Lewis acid sites and weaker metal–support interactions.<sup>118</sup>



**Scheme 14** Main paths for the catalytic hydrogenation of fumaric and succinic acid to  $\gamma$ -butyrolactone, tetrahydrofuran and 1,4-butanediol.<sup>129</sup>

### 3.2 Rhenium-promoted catalysts

Although the promise of Re-promoted catalysts was first outlined in the 1960's,<sup>119,120</sup> and followed by studies in the early 1980's which recognised the ability of rhenium heptoxide at forming synergistic combinations with other metals (*e.g.* Pd, Pt, Rh, Ru),<sup>105</sup> the interest in applying such systems for carboxylic acid hydrogenation was mainly revived in the 2000's. One of the first applications of Re-promoted catalysts was the hydrogenation of fumaric acid. This reaction was particularly challenging due to the necessity to control the distribution of reaction products that can include succinic acid,  $\gamma$ -butyrolactone (GBL) and tetrahydrofuran (THF) apart from the diol (Scheme 14).<sup>121,122</sup> This exemplifies a particular challenge of the dicarboxylic acid reduction, where intermediate formation of lactones, followed by partial reduction to cyclic ethers can completely inhibit the reduction to diols. For instance, kinetic studies<sup>123</sup> using an Ru–Re catalyst indicated the formation of GBL and THF as main products under semi-batch conditions (250–270 °C). Analysis of the rate parameters revealed that subsequent hydrogenation reactions could only proceed once the concentration of fumaric acid approached a minimum and after sufficient amounts of succinic acid had been formed.

The hydrogenation of aqueous 5%<sub>wt</sub> succinic acid to 1,4-butanediol using Re-promoted catalysts was studied by Espeel and co-workers<sup>124</sup> Prepared by impregnation or surface reduction techniques, Re–Pd/TiO<sub>2</sub> catalysts reduced in H<sub>2</sub> at 450 °C were effective in selective 1,4-butanediol production at a relatively low temperature of 160 °C. Characterisation of catalysts prepared by surface redox reaction of the Re precursor with monometallic Pd catalyst evidenced a good dispersion of Pd and Re although the authors did not investigate the oxidation state of two metals. Previous detailed characterisation studies<sup>125–128</sup> have underpinned the difficulty of reaching the full reduction of Re to the metallic state due to its high oxophilicity; such studies indicate that Re is present as ReO<sub>x</sub> species next to metallic Pd on titania. Interestingly, the amount of Re needed to induce the Pd–Re synergy can vary nearly 5-fold depending on the catalyst preparation method. Re loadings of at least 3.5%<sub>wt</sub> were required when the catalyst was prepared by impregnation compared to only 0.6–0.8%<sub>wt</sub> for the surface redox preparation.

The monometallic Pd catalysts studied by Espeel and co-workers<sup>124</sup> were mainly selective for GBL. Addition of Re to Pd/TiO<sub>2</sub> resulted in complete conversion of succinic acid and GBL with the selectivity to 1,4-butanediol over 80% with shorter reaction times. In other work,<sup>130</sup> addition of Re to carbon-supported Ru and Pt catalysts allowed to achieve increased

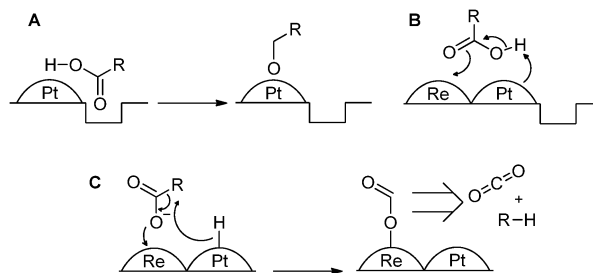


conversion of succinic acid to 1,4-butanediol under batch conditions (160–180 °C, 150 bar H<sub>2</sub>), with 1,4-butanediol selectivity and yield exceeding 60%. No significant loss of performance was observed during catalyst recycling. Again, high Re loadings were needed to induce the synergy between Pt/Ru and Re. The improved selectivity was attributed to the reduced contribution of dehydration reactions resulting in alkane by-products. The extent of alloying between the metals was brought into question with TEM measurements, which revealed a bimodal particle size distribution for 4%<sub>wt</sub> Re–2%<sub>wt</sub> Ru/C catalyst, represented by small (2–3 nm) Ru-rich particles and large (15–60 nm) particles with Ru–Re or Re-only composition.

The general promotional effect of Re in bimetallic catalysts is exemplified by Dumesic and co-workers,<sup>131</sup> who examined the hydrogenolysis of cyclic ethers to their corresponding diols using both experimental and theoretical tools. A 4%<sub>wt</sub> Rh–ReO<sub>x</sub>/C (1:0.5) catalyst was found to promote the key reaction steps: acid-catalysed ring opening, cracking and hydrogenation over bifunctional acid sites formed by the close contact of Rh and Re species. In terms of performance, moderate conversion of 2-(hydroxymethyl)-tetrahydropyran and 97% selectivity to 1,6-hexanediol was achieved in water using a flow reactor at mild conditions (120 °C, 34 bar H<sub>2</sub>). This work emphasizes the importance of hydroxyl groups, specifically those associated with oxophilic Re in close proximity to Rh atoms. Such Re–OH groups are considered to exhibit a pronounced Brønsted acidity. They are proposed to assist at the key steps of the reaction mechanism involving proton transfer to the cyclic ether and formation of the carbenium transition states leading to the selective formation of diol. Recent works by Tomishige<sup>132</sup> and Hardacre<sup>103,133</sup> further demonstrated the versatility of Re-containing catalysts for the hydrogenation of C<sub>6</sub>–C<sub>18</sub> fatty acids including hexanoic, capric, palmitic and stearic acids. Using a ReO<sub>x</sub>–Pd/SiO<sub>2</sub> (Pd/Re = 1:8 molar) catalyst, fatty alcohol yields in excess of 92% were obtained for all fatty acids investigated after 16–24 hours reaction (140 °C, 80 bar H<sub>2</sub>).<sup>132</sup> For shorter chain fatty acids including hexanoic and octanoic acid, alcohol yields exceeded 98% and only trace amounts of alkane products were observed due to the suppression of both fatty acid decarboxylation and fatty alcohol dehydration.

Interestingly, Tomishige found that Pd/SiO<sub>2</sub> had no activity for stearic acid hydrogenation while marginal activity was demonstrated by ReO<sub>x</sub>/SiO<sub>2</sub>. It was therefore proposed that the activity was defined by ReO<sub>x</sub> rather than Pd species. This contrasted the findings of Hardacre,<sup>103</sup> who encountered the opposite alcohol selectivity trend for Pt–Re/TiO<sub>2</sub> (60–80%) and monometallic Pt/TiO<sub>2</sub> (93%) catalysts in stearic acid hydrogenation. This reaction was successfully carried out at 120 °C with only 20 bar H<sub>2</sub> pressure – the conditions that were unprecedentedly mild at the time of publication. The addition of Re to Pt/TiO<sub>2</sub> resulted in a strong enhancement of the hydrogenation activity and partially decreased the alcohol selectivity giving rise to alkane by-products. Selectivity to stearyl alcohol did not correlate with Re content, however, the rate of reaction increased with Re loading up to a value of 4%<sub>wt</sub>.

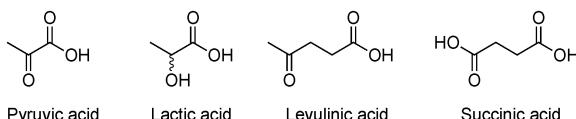
Major by-products of stearic acid hydrogenation comprised C<sub>17</sub> alkanes formed *via* the decarboxylation of stearic acid.



**Scheme 15** Proposed mechanism for the hydrogenation of carboxylic acids over Pt and Pt–Re/TiO<sub>2</sub> surfaces and contrasting (A) the interaction of the oxygen atoms of the carbonyl group with supported oxygen vacancies created by hydrogen spillover facilitated by Pt, (B) the specific interaction of the carbonyl group with Pt and Re, and (C) the decarboxylation of carboxylic acid molecules over Re atoms in Pt–Re/TiO<sub>2</sub>.<sup>103</sup>

Taking into account previous findings reported by Mendes *et al.*,<sup>113</sup> several mechanisms were proposed to account for the product selectivities over Pt and Pt–Re sites on TiO<sub>2</sub> (Scheme 15). For Pt/TiO<sub>2</sub> catalysts, the formation of Ti<sup>4+</sup> defects/oxygen vacancies was viewed as essential for activating the carbonyl group while Pt facilitated the hydrogenation reaction. For bimetallic Pt–Re catalysts, the presence of highly oxophilic Re centres may facilitate the hydrogenation of carboxylic acids to form alcohols and alkanes *via* different mechanisms also involving the interaction with the oxygen atom of the carbonyl group. A subsequent study<sup>133</sup> employed *in situ* EXAFS measurements to shed light on the interplay between the catalyst activity, Pt–Re interactions and the involvement of reaction solvent and the catalyst support. Experiments were designed to evaluate reduction phenomena in both liquid and gas phases, with gas phase reaction concluded to be a more efficient approach. Interestingly, the choice of solvent (THF vs. hexane) was proposed to influence the metallic character of the catalyst, albeit to a minimal extent. However, significant differences were observed when reducing Pt and Re metals on Al<sub>2</sub>O<sub>3</sub> and TiO<sub>2</sub> supports. TiO<sub>2</sub> allowed a more efficient reduction of the supported metal species. In addition, supported Pt–Re catalysts applied in hydrogenation of stearic acid<sup>103</sup> were observed to lose activity upon their reuse due to the formation of surface carbonaceous residue *in situ*. Metal leaching, however, was found to be negligible and it was shown that the original activity of these catalysts could be restored by calcination and reduction in sequence. A partial regeneration of catalytic activity may also suggest the effect of hydrogenation reaction on Pt–Re interactions.

An extraordinary oxophilicity of Pt–Re catalysts render them highly potent C=O reduction catalysts. Particular examples include highly active and selective amide hydrogenation catalysts, that produce tertiary amines from tertiary amides<sup>134–136</sup> with no C–N cleavage that is typical for homogeneously catalysed amide reduction.<sup>137</sup> A large number of substrates were recently screened by Breit and Stein<sup>134</sup> under mild conditions (ca. 160 °C, 5–70 bar H<sub>2</sub>) using a 2% Pt–10% Re/graphite catalyst. For a series of cyclic amides more than 99% conversion and excellent selectivity toward the tertiary amine product was achieved. This reactivity of Pt–Re and other catalysts for the hydrogenation of



Scheme 16 Selected examples of carboxylic acids containing reactive functional groups.

carboxamides has been discussed in great detail in a recent review by Smith and Whyman.<sup>20</sup>

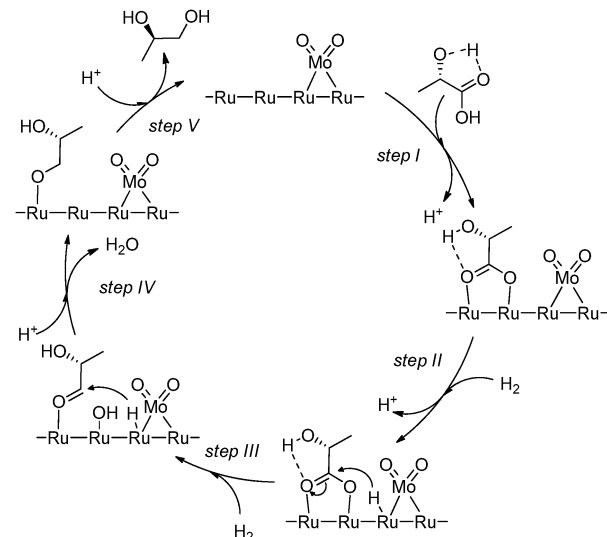
### 3.3 Hydrogenation of functionalized and biomass-derived carboxylic acids

A special focus with respect to catalytic reduction should be laid on functionalized carboxylic acids. Many of these substrates are derived from renewable sources and their conversion is an important step in production of platform chemicals from sustainable feedstock. Functionalized acids typically bear additional oxygen-containing functional groups. Most typical examples include  $\alpha$ -hydroxy-,  $\alpha$ -keto-,  $\gamma$ -ketoacids and dicarboxylic acids such as lactic, pyruvic, levulinic and succinic acids respectively (Scheme 16). Ultimately, the complete catalytic hydrogenation of such compounds should yield 1,2- and 1,4-diols as final products. If the two alcohol groups are far apart in the substrate, side reactions such as formation of lactones can take place depending on the type of catalyst and reaction conditions applied. These trends were described above for the succinic acid hydrogenation and remain valid for other substrates outlined in the Scheme 16.

Hydrogenation of the  $\alpha$ -carbonyl function commonly does not present a challenge for catalysis. For example, conversion of pyruvic acid to lactic acid can be performed at 100 °C under 10 bar H<sub>2</sub> pressure using Ru/starbon catalysts.<sup>138</sup> Further hydrogenation of lactic acid to 1,2-propanediol requires significantly harsher conditions. One of the first reports by Miller and co-workers<sup>139</sup> presented a series of supported Ru catalysts capable of selective hydrogenation at mild temperatures (100–170 °C) and elevated H<sub>2</sub> pressures (70–140 bar). It was possible to convert more than 95% of the lactic acid feed into propylene glycol with over 90% selectivity using a Ru/C catalyst. Both lactic acid conversion and propylene glycol selectivity increased until 150 °C. At higher temperatures the propylene glycol yield decreased due to alcohol dehydration. This catalyst also allowed efficient hydrogenation of other glucose fermentation products such as calcium lactate salts without a significant loss of the catalyst performance.

Using MoO<sub>x</sub>-doped Ru/C catalyst, Tomishige and co-workers<sup>140</sup> very recently managed to improve the reaction conditions reaching near quantitative yields of propanediol in hydrogenation of lactic acid at 80 °C under 80 bar H<sub>2</sub> pressure. Authors demonstrated a four-fold increase in TOF (up to 114 h<sup>-1</sup>) upon addition of MoO<sub>x</sub> to the Ru/C catalyst and proposed a reaction mechanism for the hydrogenation (Scheme 17).

The reaction is initiated by the adsorption of the acid on Ru surface in the form of a carboxylate intermediate (I, Scheme 17). The next step, proposed to take place on Ru/MoO<sub>x</sub> pair, involves



Scheme 17 Mechanism of lactic acid hydrogenation to 1,2-propanediol over Ru-MoO<sub>x</sub>/C catalyst proposed by Tomishige and co-workers.<sup>140</sup>

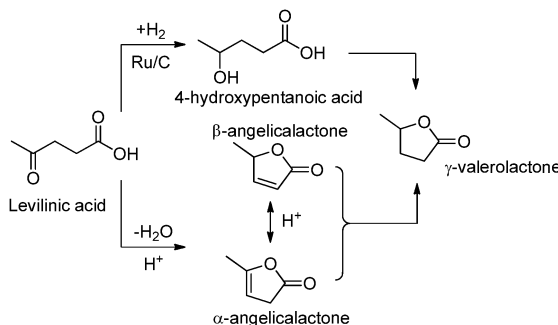
heterolytic dissociation of H<sub>2</sub> that yields Ru hydride (II). The hydride attack of the carbonyl carbon of the carboxylate and subsequent C–O cleavage yields the aldehyde intermediate which is then further hydrogenated in step (IV). The last step involves desorption of the alkoxy species from Ru to yield the propanediol product.

Authors argue that adsorption of the substrate takes place on Ru surface, while for related Rh–MoO<sub>x</sub>/SiO<sub>2</sub> catalysts applied for ether hydrogenolysis the substrates are mainly adsorbed on MoO<sub>x</sub>.<sup>141</sup> This difference is explained in part by the relatively low Mo/Ru ratio (1:16) necessary to achieve the optimum performance of the acid-hydrogenation bimetallic catalyst.

Finally, very recent works by Li and co-workers<sup>142</sup> on Ir-catalysed hydrogenation of carboxylic acids also clearly demonstrated the efficiency of MoO<sub>x</sub> promotion. Bimetallic Ir–MoO<sub>x</sub>/SiO<sub>2</sub> catalysts were superior to their monometallic analogues in lactic and succinic acid hydrogenation at 100 °C and 60 bar H<sub>2</sub> pressure.

The hydrogenation of the carboxylic group in  $\alpha$ -oxygenated carboxylic acids is usually straightforward.<sup>143</sup> However, a more complex reactivity can be encountered for the conversion of bio-derived  $\gamma$ -ketoacids.<sup>144,145</sup> The formation of intermediate products such as lactones can be encountered for substrates, containing more than one functional group. Indeed, lactones have been observed during the hydrogenation of levulinic acid (Scheme 18).<sup>146–148</sup> The major product of this reactions is  $\gamma$ -valerolactone (GVL), which can be produced *via* two reaction pathways, the first of which proceeds *via* hydrogenation of the ketone group in levulinic acid to form 4-hydroxypentanoic acid (HPA) followed by acid-catalysed dehydration and ring closure to produce GVL. The second pathway involves the dehydration of levulinic acid to form angelicalactones, which can then be hydrogenated to GVL (Scheme 18). A prominent example of selective reduction of LA to GVL is a recently reported study by the group of Weckhuysen<sup>149</sup> who used a set of 1%<sub>wt</sub> Pd–Ru/TiO<sub>2</sub>





Scheme 18 Generation of  $\gamma$ -valerolactone (GVL) via hydrogenation of levulinic acid.<sup>146</sup>

catalysts prepared *via* a modified impregnation ( $M_{Im}$ ) route involving addition of excess chloride ions. Such catalysts allowed achieving both high activity ( $TOF = 0.6\text{ s}^{-1}$ ) and stable 99% selectivity towards GVL at  $200\text{ }^\circ\text{C}$ . Authors proposed that Pd promotes the dilution and isolation of active Ru sites, introducing a stabilization effect and thereby preventing the consecutive hydrogenation of the GVL product. Non-noble metals, *e.g.* Ni, can also be used for production of GVL. Rao and co-workers<sup>150,151</sup> recently reported 100% LA conversion and 85% GVL selectivity attainable with supported Ni catalysts operating at  $250\text{--}300\text{ }^\circ\text{C}$  in vapour phase. Related transformations of oxygenated carboxylic acids have been studied in great detail and discussed in a recent review by Pinel and co-workers.<sup>152</sup>

Further hydrogenation of GVL leading to the formation of 1,4-pentanediol requires harsher conditions to proceed and typically bimetallic catalysts are employed for this transformation. Cong and co-workers<sup>153</sup> studied the activity of Rh/SiO<sub>2</sub> catalysts doped with MoO<sub>x</sub> in this reaction. Starting from aqueous levulinic acid, authors achieved nearly full acid conversion and good 1,4-pentanediol (PDO) yields up to 70% at temperatures as low as  $80\text{ }^\circ\text{C}$ . The synergy between Rh and MoO<sub>x</sub> was confirmed by referencing the activity of the bimetallic catalysts against one of their monometallic counterparts. Under the same conditions, full conversion of aqueous acetic acid with 83% ethanol selectivity could be obtained. As a result, this work sets a benchmark in terms of the reaction temperature, required to hydrogenate carboxylic acids to alcohols.

Promotion of the noble metal catalysts (*e.g.* Pd, Pt, Ru) by Re was also shown to result in highly active catalysts for hydrogenation of LA and GVL. By using a 1.9%<sub>wt</sub> Ru 3.6%<sub>wt</sub> Re/C catalyst, Pinel and co-workers achieved the diol selectivity of 82% when LA hydrogenation was performed at  $140\text{ }^\circ\text{C}$  under 150 bar H<sub>2</sub> pressure.<sup>154</sup> Remarkably this reaction was performed in aqueous media.

Apart from Mo or Re doping, one can employ a metal-support bifunctional catalyst for 1,4-PDO production. A remarkable example reported by Fan and co-workers<sup>155</sup> describes the use of Cu/ZrO<sub>2</sub> catalyst that allows more than 97% 1,4-PDO yields in hydrogenation of GVL at  $200\text{ }^\circ\text{C}$  under 60 bar H<sub>2</sub> pressure. This catalyst was shown to be stable upon recycling and exhibited no apparent activity loss when reused three times.

Significantly higher reaction temperatures are required to transform levulinic acid or GVL into alcohols using conventional monometallic catalysts. For example, early examples of Cu/Cr<sub>2</sub>O<sub>3</sub> catalysts reported in 1947 by Christian *et al.*<sup>156</sup> could provide high yields of 1,4-pentanediol (>70%) in hydrogenation of pure GVL, ethyl levulinate or levulinic acid only at  $250\text{ }^\circ\text{C}$  and 200 bar H<sub>2</sub> pressure. Noble metal Ru/C catalyst also require harsh operating conditions ( $190\text{ }^\circ\text{C}$  and 120 bar H<sub>2</sub> pressure) to produce 2-methyl tetrahydrofuran in hydrogenation of GVL. Copper catalysts developed later by Luque and co-workers<sup>157</sup> perform better than Ru/C systems but also generate mainly 2-methyl tetrahydrofuran with PDO formed with only 25% selectivity.

### 3.4 Outlook

The number of heterogeneous catalysts successfully applied for the hydrogenation of carboxylic acid derivatives to corresponding alcohols has grown substantially in recent years. The best reported heterogeneous catalysts are comprised of noble metals in combination with Sn, Mo and Re promoters. The bimetallic composition of these catalysts was demonstrated to be responsible for the activity and selectivity control that is mainly associated with the activation of the carboxylic acid group.

Apart from the metallic additives, the catalyst support itself may act as the promoter and assist in the substrate activation steps or even utilize solvent molecules in catalytic transformations. Therefore, a heterogeneous catalysis researcher ultimately deals with cooperative tri-component systems with vast tuning versatility.

Although rarely discussed in the same framework, the cooperative effects in heterogeneous systems resemble closely ones encountered in homogeneous catalysis. Therefore, in the next part of this review we will address the ester hydrogenation from a homogeneous perspective to highlight the common features of the catalysts developed in these different research fields.

## 4. Homogeneous catalysis in hydrogenation of carboxylic acid esters and lactones

Heterogeneously catalysed hydrogenation of carboxylic acid derivatives is mainly focused at the conversion of biomass-derived substrates such as oils and fats, GVL and levulinic acid. On the other hand, homogeneous catalysts have a substrate scope significantly broader than that of their heterogeneous counterparts. Apart from aliphatic, aromatic esters and lactones, some homogeneous catalysts are capable of hydrogenating substrates containing chiral centres, various reducible groups or heteroatom functions. Modern state-of-the-art homogeneous catalysts typically operate at significantly lower temperatures than their heterogeneous counterparts, thereby allowing for an exclusive selectivity towards alcohol product. Hydrogenation of carboxylic acid derivatives using homogeneous catalysts has

been previously described as a part of several comprehensive reviews.<sup>19,137,158,159</sup> Therefore, we will limit the discussion in the current review to the milestone achievements in the field while also discussing the latest developments in ester hydrogenation catalysis in more detail. A special emphasis will be placed on the mechanistic works, addressing catalytic hydrogenation of esters. Similarities between bifunctional hetero- and homogeneous catalysts will also be discussed in an attempt to bridge these two fields.

#### 4.1 Early works and the TriPhos catalysts

One of the first examples of a homogeneous catalyst for the hydrogenation of activated esters was reported in 1980 by Grey and Pez.<sup>160–162</sup> Methyl and trifluoroethyl trifluoroacetate esters were hydrogenated to corresponding alcohols with good yields (>88%) at 90 °C and 6 bar H<sub>2</sub>. A potassium hydridophosphine ruthenate complex K<sub>2</sub>[(Ph<sub>3</sub>P)<sub>3</sub>(Ph<sub>2</sub>P)Ru<sub>2</sub>H<sub>4</sub>]<sub>2</sub>(C<sub>6</sub>H<sub>14</sub>O<sub>3</sub>) was used in these studies at approx. 0.3%<sub>mol</sub> loading with respect to the ester substrate. Several years later, Piacenti and co-workers reported the first hydrogenation of a non-activated ester substrate.<sup>163</sup> Using a Ru(CO)<sub>2</sub>(CH<sub>3</sub>COO)<sub>2</sub>(PBu<sub>3</sub>)<sub>2</sub> complex, the authors achieved full conversion in the hydrogenation of dimethyl oxalate to methyl glycolate. However, the reaction required high temperature and pressure (180 °C, 132 bar H<sub>2</sub>) and further hydrogenation of methyl glycolate to ethylene glycol was hampered. In 1991, Hara and Wada reported the hydrogenation of anhydrides and lactones using a catalyst formed *in situ* from Ru(acac)<sub>3</sub> and trioctylphosphine.<sup>164,165</sup> A substantial improvement of the catalyst performance in the presence *p*-toluenesulfonic acid (PTSA) or H<sub>3</sub>PO<sub>4</sub> additives was reported for the hydrogenation of  $\gamma$ -butyrolactone to 1,4-butanediol (200 °C, 50 bar H<sub>2</sub>).

Early examples of ester hydrogenation catalysts utilized high operating temperatures and pressures. A major improvement in this respect was achieved by Teunissen and Elsevier with the introduction of TriPhos type of ligands.<sup>166</sup> They applied a TriPhos<sup>Ph</sup> ligand in combination with Ru(acac)<sub>3</sub> in dry methanol for the hydrogenation of dimethyl oxalate and achieved *ca.* 95% yield of ethylene glycol under optimized conditions. The performance of the catalyst operating at 100–120 °C and under 70 bar H<sub>2</sub> pressure was enhanced by the introduction of metallic zinc. This accelerated the reduction of the initial Ru<sup>3+</sup> species, thereby enabling a fast precatalyst formation. Using the same approach, the hydrogenation of aromatic and aliphatic esters was further developed<sup>167</sup> with a particular focus on the hydrogenation of dimethyl phthalate, a substrate, at that time, had only a single previous example of catalytic hydrogenation.<sup>168</sup> The performance of Elsevier's catalytic system in dimethyl phthalate hydrogenation strongly depended on additives and while the addition of zinc deteriorated the catalytic activity, promoters such as NEt<sub>3</sub> and HBF<sub>4</sub> significantly increased alcohol yield. Ultimately, a 78% yield of 1,2-bis(hydroxymethyl)-benzene was achieved using 1.5%<sub>mol</sub> catalyst in <sup>1</sup>PrOH solvent in combination with HBF<sub>4</sub> at 85 bar H<sub>2</sub> pressure and 100 °C.

Although harsh operating conditions still represent a major drawback of the TriPhos system, a number of works recently

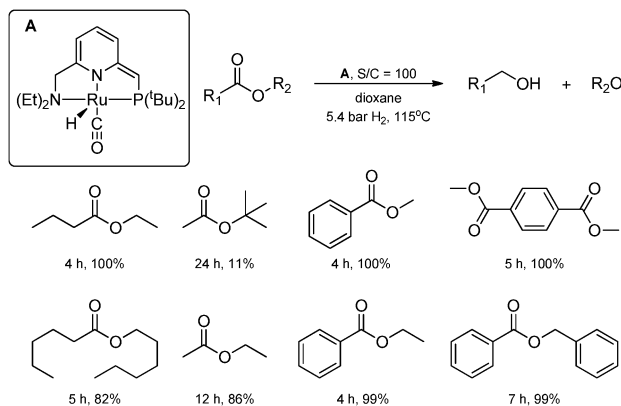
reported its improved performance for the hydrogenation of non-activated esters and dicarboxylic acids.<sup>169–171</sup> The latter is particularly interesting, since the examples of homogeneously-catalyzed hydrogenation of free carboxylic acids are scarce. Studies by Leitner and co-workers established the activity of the Ru/TriPhos system for the hydrogenation of levulinic (LA) and itaconic (IA) acids. These biogenic substrates could be converted into diols, lactones and cyclic ethers depending on the ligands and additives used. Typically, operating at 160–200 °C and under 100 bar H<sub>2</sub> pressure, the researchers managed to fully convert both IA and LA. The major product (96% yield) of IA hydrogenation in the presence of PTSA and NH<sub>4</sub>PF<sub>6</sub> was 3-methyltetrahydrofuran, while 2-methylbutanediol was formed selectively when no additives were present. A similar trend was observed for LA hydrogenation, which yielded  $\gamma$ -valerolactone under additive-free reaction conditions and 2-methyltetrahydrofuran in the presence of NH<sub>4</sub>PF<sub>6</sub> and sulfonated ionic liquid.<sup>172</sup> These important examples demonstrate the utility of Ru/TriPhos catalysts for very selective reduction of acids with a possibility to alter the final product by choosing specific additives.

#### 4.2 Bifunctional homogeneous catalysts for ester hydrogenation

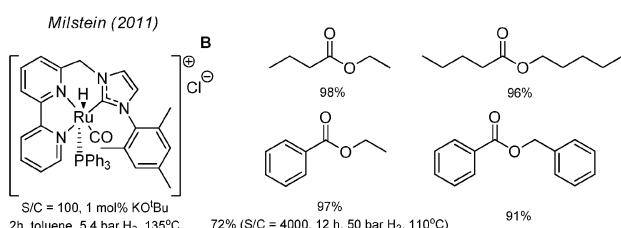
Similar to heterogeneous catalysis, the majority of active homogeneous ester hydrogenation catalysts are bifunctional. The first example of such catalysts for the hydrogenation of esters was reported in 2006 by Milstein and co-workers.<sup>173</sup> A ruthenium lutidine-based 16-electron pincer complex **A** (Scheme 19) was able to hydrogenate a broad range of non-activated esters at a relatively mild temperature of 115 °C and a low H<sub>2</sub> pressure of only 5.4 bar. The major improvement, associated with the use of **A**, was the possibility of operation under neutral conditions without additives. The bifunctional action of Milstein's catalyst relied on the reversible aromatization/dearomatization of the pyridine ligand backbone in **A**.<sup>174</sup> In the dearomatized state, complex **A** contained an acid–base pair consisting of a metal centre and a deprotonated ligand sidearm, which was found to act in a concerted manner to activate H<sub>2</sub> through a heterolytic mechanism (Scheme 19).

The class of bifunctional pincer catalysts based on ligands with aromatic backbones was further expanded with the use of N-heterocyclic carbene (NHC) ligands. Milstein and co-workers reported a ruthenium CNN-pincer **B** (Scheme 20) based on a bipyridine backbone.<sup>175</sup> In the presence of 1%<sub>mol</sub> KO'Bu, complex **B** was able to convert aromatic and aliphatic esters at 135 °C under 5.4 bar H<sub>2</sub> pressure. Simultaneously, Song and co-workers<sup>176</sup> presented an Ru–CNN pincer complex **C** resulting from the incorporation of the NHC donor group instead of phosphine in the original Milstein Ru–PNN catalyst **A**. The resulting pincer catalyst exhibited hydrogenation activity superior to that of the phosphine-based analogue **A**. At 105 °C and under 5.3 bar H<sub>2</sub> pressure, catalyst **C** required at least two-fold shorter reaction times to achieve similar levels of conversion. The use of bis-NHC pincer complexes for ester hydrogenation was recently reported by our group.<sup>177</sup> The Ru–CNC pincer



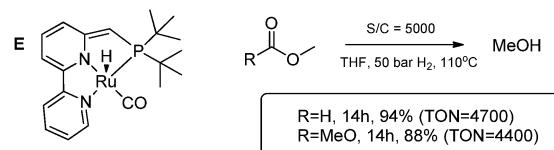


**Scheme 19** Performance of Milstein's lutidine-based Ru-PNN catalyst **A** in ester hydrogenation.

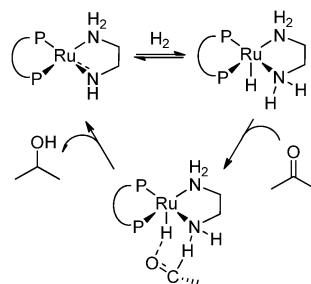


**Scheme 20** Performance of NHC-based ruthenium pincer catalysts in ester hydrogenation.

complex **D** was capable of producing up to 1000 turnovers in methyl benzoate hydrogenation at 70 °C under 50 bar H<sub>2</sub> pressure. Finally, in 2011, Milstein and co-workers reported an outstanding Ru-PNN pincer catalyst **E** for hydrogenation of organic carbonates and formates.<sup>25</sup> The best performance was achieved in THF solvent at 110 °C under 50 bar H<sub>2</sub> pressure. At catalyst loadings of only 0.02%<sub>mol</sub>, **E** (Scheme 21) promoted the hydrogenation of methyl formate and dimethyl carbonate to



**Scheme 21** Hydrogenation of methyl formate and dimethyl carbonate using catalyst **E**.<sup>25</sup>



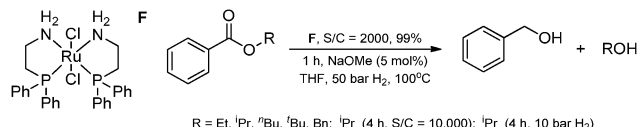
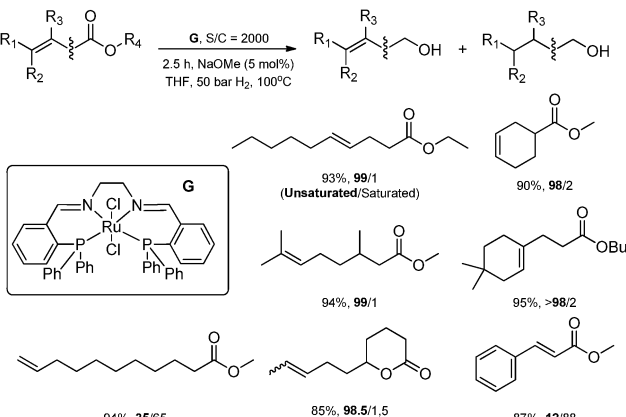
**Scheme 22** Selected steps of cooperative hydrogenation according to Noyori–Morris mechanism.

methanol with 94 and 88% yields, respectively, with TON values of over 4400.

A common feature of catalysts **A–E** is the bifunctional behaviour based on the reversible aromatization/dearomatization of the ligand backbone, and this type of bifunctional catalysts has been recently reviewed by Milstein and co-workers.<sup>31</sup> A second large class of ester hydrogenation catalysts showing a pronounced bifunctional behaviour was originally developed by Noyori,<sup>178</sup> Morris,<sup>179,180</sup> Ikariya<sup>181</sup> and Gao<sup>182</sup> for highly efficient hydrogenation of ketones and imines.<sup>178,181,183,184</sup> Typical catalysts of this type contain bidentate (N,N), (P,P) or hybrid (N,P) ligands and rely on reversible amine/amide transformation that forms the basis for their bifunctional behaviour. Generally speaking, such behaviour (Scheme 22) requires a ruthenium amide function that assists in H<sub>2</sub> cleavage over the Ru–NR bond. An Ru amino hydride complex, produced in this reaction, contains RuH<sup>δ-</sup> and NRH<sup>δ+</sup> groups that can interact with, and hydrogenate substrates in the second coordination sphere. Subsequent concerted transfer of the hydride and proton to carbonyl group of the substrate regenerates the initial amido complex and yields the hydrogenated product.

The presence of the cooperative amine function in the immediate vicinity to the metal centre typically results in more active ester hydrogenation catalysts when compared to Milstein-type systems. The first example of catalytic hydrogenation of esters using Noyori-type catalysts was reported by Sudan *et al.*<sup>185</sup> Among several ruthenium complexes with chelating (N,P) and (P,N,N,P) ligands, catalysts **F** and **G** (Schemes 23 and 24) were the most active. Remarkable performance in the hydrogenation of a wide range of benzoic acid esters was exhibited by catalyst **F** (Scheme 23). Both rapid and near complete conversion was found to be possible using mild conditions and very low catalyst loadings (0.1–0.01%<sub>mol</sub>).



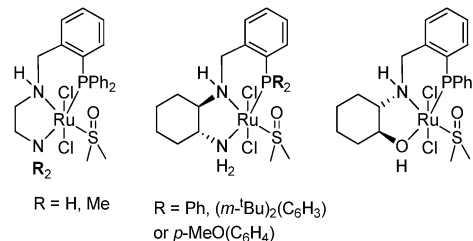
Scheme 23 Hydrogenation of benzoic acid esters using catalyst F.<sup>185</sup>Scheme 24 Chemoselective hydrogenation of esters using catalyst E.<sup>185</sup>

The performance of catalyst **F** was also superior to that of previously described pincer complexes **A–D** as well as TriPhos-based systems, although direct comparison of the catalysts is complicated due to the different nature of the substrates and variation in reaction conditions. The maximum TON value obtained over **F**, is *ca.* two-fold higher than that of the most active Milstein-type catalyst **E**.

Probably the most striking improvement made by Saudan *et al.* was the disclosure of the chemoselective hydrogenation of esters using catalyst **G** (Scheme 24). Here, authors overcame a typical problem of active hydrogenation catalysts, that is, the intolerance to other reducible functionalities such as carbon–carbon double bonds. They demonstrated that the degree of substitution at the double bond and its location could directly influence the chemoselectivity of the reduction. Whereas internal alkene functionality could be preserved, terminal alkenes and  $\alpha,\beta$ -unsaturated substrates lost their olefin function during hydrogenation. Authors further demonstrated that the ester reduction path is kinetically preferred over the olefin reduction. This fact suggests that it may be possibility to improve the yields of unsaturated alcohols through optimisation of the process conditions.

Following this breakthrough, the performance of the Noyori-type catalysts was explored by Clarke and co-workers,<sup>186</sup> who developed a convenient procedure for hydrogenation of various esters at near-ambient temperature using isolated or *in situ* formed Ru catalysts with bi- and tridentate aminophosphine ligands (Scheme 25).

Another class of exceptionally active ester hydrogenation catalysts is based on amino-pincer ligands. The major difference with conventional Noyori type catalysts is the presence of three donor groups in the ligand that bind in a *meridional* manner.

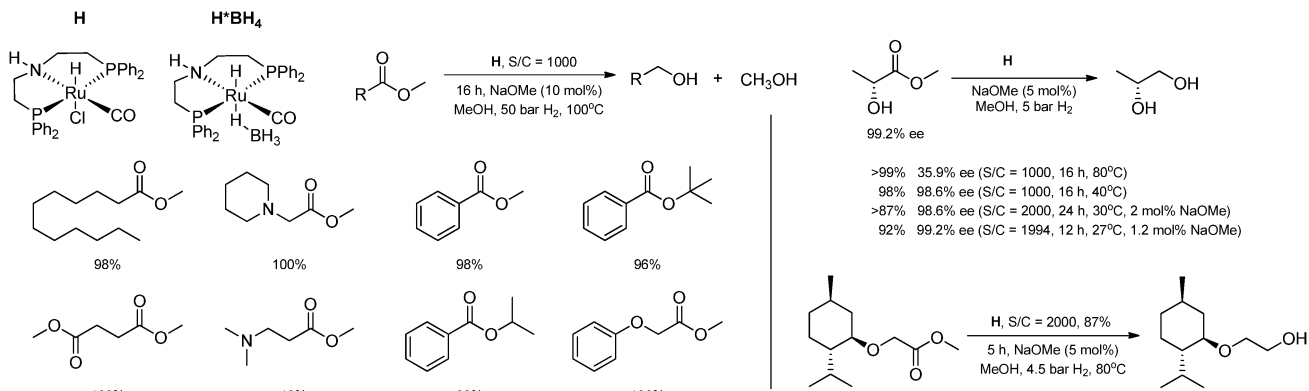
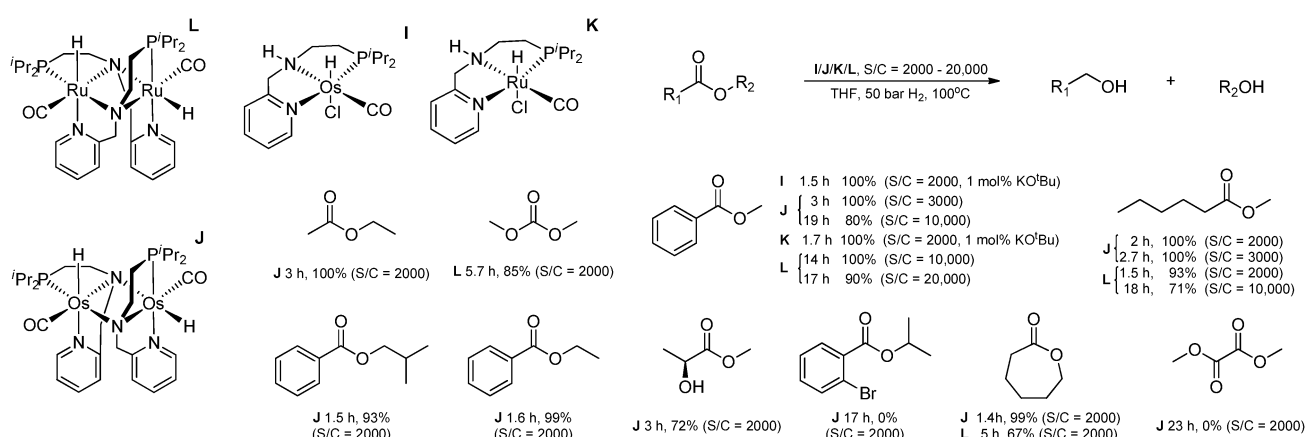
Scheme 25 Examples of Ru-PNN and PNO catalysts of Clarke and co-workers.<sup>186</sup>

The presence of amino pincer ligands is responsible for the bifunctional nature of these catalysts as illustrated by the reports from the groups of Grützmacher<sup>187</sup> and Schneider.<sup>188</sup> One of the first examples of an amino pincer catalyst for ester hydrogenation was reported in 2011 by Saito and co-workers from Tagasako corp. They disclosed catalyst **H** (Scheme 26) – a system specifically designed for industrial applications.<sup>189</sup> The catalyst tolerated methanol solvent that simplified the workup of methyl ester hydrogenation reactions. At S/C = 1000–2000, catalysts **H** and **H\*BH4** were active in hydrogenation of aromatic, aliphatic and chiral esters (Scheme 26). For example, 2-((*L*)-menthoxymethyl)ethanol was obtained in 87% yield from the corresponding methyl ester at S/C = 2000. Importantly, catalyst **H\*BH4** also efficiently converted the protected  $\alpha$ - and  $\beta$ -amino acids into corresponding amino alcohols with negligible loss of optical purity.

The current state of the art catalysts for the hydrogenation of esters were developed by Gusev and co-workers. In 2012, authors introduced a family of Ru and Os PNN-pincer catalysts based on picolylamine-derived backbone with a phosphine donor group attached to it *via* an ethylene linker (**I–L**, Scheme 27).<sup>190</sup> A wide range of aliphatic and aromatic esters were hydrogenated in good to quantitative yields at S/C = 2000. An outstanding TON value of 20 000 for the most active Ru-PNN catalyst **L** in hydrogenation of methyl benzoate was achieved. Catalysts **I–L** also showed activity in hydrogenation of triglycerides and with partial preservation of the olefin functionality in case of oleic acid esters. Typical operation using catalysts **I–L** required temperatures of 100 °C and 50 bar H<sub>2</sub> pressure.

Further research by the same group led to the development of a family of Ru-SNS pincer catalysts<sup>191</sup> (Scheme 28) structurally similar to Takasago catalyst **H**. The most active of them, catalyst **M**, currently holds the record in ester hydrogenation activity with unprecedented turnover numbers up to 58 400 achieved in hydrogenation of neat ethyl acetate at only 40 °C. A rough estimation of hydrogenation TOF (turnover frequency) gives a value of 4900 h<sup>-1</sup> for a 2 hour experiment (100 °C, 50 bar H<sub>2</sub>) using methyl hexanoate as a model substrate (Scheme 27). Due to the combination of its high activity and ease of preparation, Gusev's Ru-SNS catalyst has been commercialised.<sup>192</sup>

Surprisingly, the aminopincer ligand platform can promote chemoselective ester hydrogenation. Very recently, Gusev and co-workers<sup>193</sup> introduced a tridentate aminopincer catalyst **N** (Scheme 29) capable of chemoselective hydrogenation of esters and unsaturated aldehydes and ketones. Outstanding selectivity

Scheme 26 Hydrogenation of esters using Ru-MACHO catalyst **H**.<sup>189</sup>Scheme 27 Ester hydrogenation by Gusev's Ru and Os PNN-pincer catalysts.<sup>190</sup>

towards ester group reduction was demonstrated for the majority of substrates tested. Catalyst **N** was active in the presence of carbonate bases, *e.g.*  $\text{K}_2\text{CO}_3$  or  $\text{Cs}_2\text{CO}_3$  that allows for the hydrogenation of substrates that do not tolerate alkoxide bases typically used in ester reduction.

Finally, a recent example of ruthenium catalyst containing a bipyridine-derived tetradentate PNNN ligand disclosed by Zhou and co-workers<sup>194</sup> set a current benchmark of the TON value attained in ester hydrogenation. Catalyst **O** (Scheme 29), operating at 25 °C, performed 91 000 turnovers in hydrogenation of  $\gamma$ -butyrolactone under 101 bar  $\text{H}_2$  pressure. Another very recent example of a tetradentate Ru-PNNP complex disclosed by Zhang and co-workers<sup>195</sup> (catalyst **P**, Scheme 30) displays a remarkable performance in hydrogenation of aliphatic and aromatic esters with some chemoselectivity observed for unsaturated esters containing the remote C=C double bonds. These recent examples place tetradentate ligands in the spotlight for future development of highly active catalysts.

In summary, we have witnessed a tremendous progress in Ru catalysis over the last years. The high stability of newly disclosed transition metal complexes results in remarkable TON values that nearly reached 100 000 (2014). The improvement in catalyst performance is, however, challenging to quantify. This obstacle mainly originates due to different reaction conditions

applied by different authors. Secondly, the substrate scopes of different catalysts rarely overlap, making it troublesome to select a single reference substrate. Nevertheless, the most common substrate – methyl benzoate, can be used to compare the performance of the state-of-the-art catalysts and illustrate the progress made in the field towards the development of highly efficient catalysts (Table 4). The scale of ester hydrogenation typically does not exceed several hundred mmol in laboratory setups; yet, several scale-up efforts have been reported. The most appealing example is the Ru-MACHO catalyst **H**, which was shown to operate at a tonne scale.<sup>189</sup> In addition, recent report by Guan and co-workers discloses the utility of a number of catalysts described in Section 4 in hydrogenation of coconut oil on a 100–1500 gram scale.<sup>196</sup>

#### 4.3 Iron pincer catalysts for ester hydrogenation

A new direction in catalytic ester hydrogenation emerged in early 2014 with the publication of three independent reports on Fe-catalysed hydrogenation of activated and non-activated esters. The group from Milstein was the first to acknowledge that “*the substitution of expensive and potentially toxic noble-metal catalysts by inexpensive, abundant, and environmentally benign metals is a prime goal in chemistry*”.<sup>197</sup> Using the dihydrido iron pincer complex **Q** with cooperative lutidine-derived PNP ligand (Scheme 31), the authors were able to hydrogenate a variety of



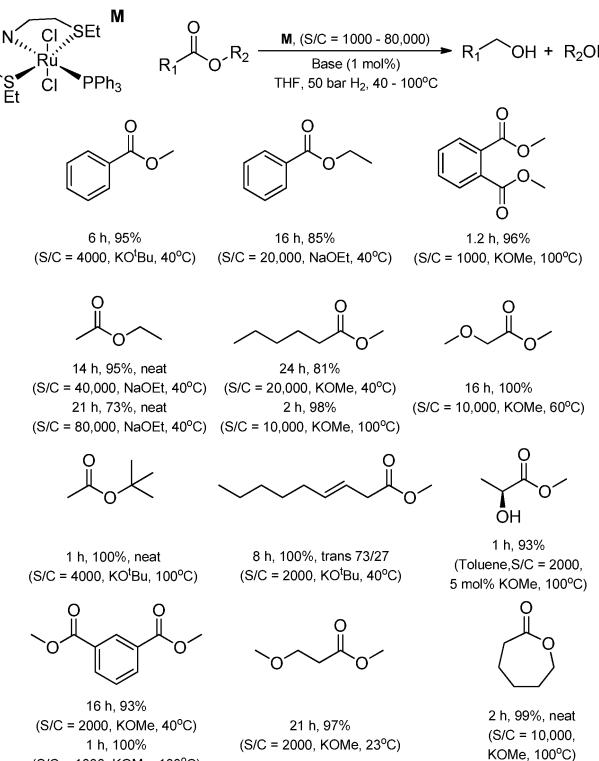
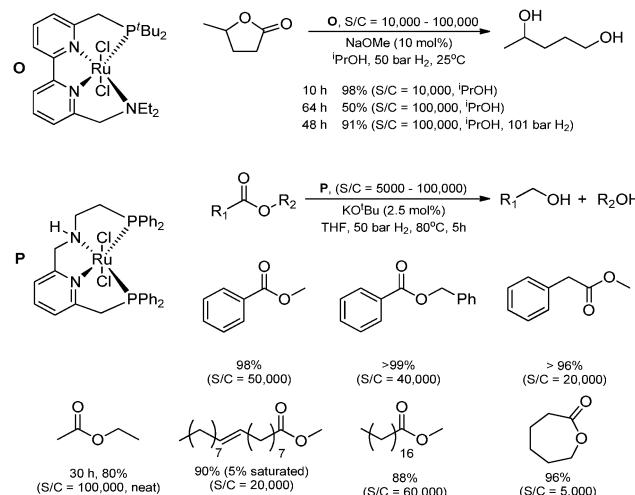
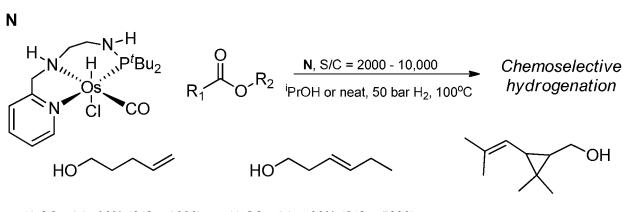
Scheme 28 Ester hydrogenation by Gusev's Ru-SNS pincer catalysts **M**.<sup>191</sup>Scheme 30 Structures and selected activity examples of tetradeinate Ru catalysts developed by Zhou (**O**)<sup>194</sup> and Zhang (**P**).<sup>195</sup>

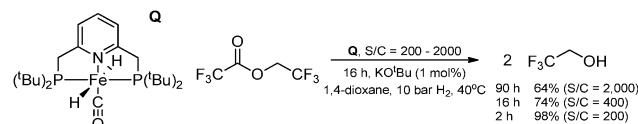
Table 4 Selected results of methyl benzoate hydrogenation using state-of-the-art Ru catalysts

Catalyst	S/C	Y (%)	T (°C)	P (bar H <sub>2</sub> )	Reaction time (h)	Ref.
<b>H</b>	1000	98	100	50	16	189
<b>K</b>	2000	100	100	50	1.7	190
<b>L</b>	20 000	90	100	50	17	190
<b>M</b>	4 000	95	40	50	6	191
<b>O</b>	100 000	91	25	101.3	64	194
<b>P</b>	50 000	98	80	50	5	195

Scheme 29 Gusev's Os catalyst **N** and examples of alcohols attainable in chemoselective ester hydrogenation with **N**.<sup>193</sup>

fluorinated esters in near quantitative yields. Hydrogenation of 2,2,2-trifluoroethyl trifluoroacetate was achieved under mild conditions (10 bar H<sub>2</sub>, 40 °C) with yields varying from 98% at S/C = 200 to 64% at elevated S/C = 2000. The hydrogenation of *n*-butyl trifluoroacetate was also attempted at S/C = 50, but was found to be considerably slower compared to 2,2,2-trifluoroethyl trifluoroacetate.

Catalyst **Q** was proven to be inactive in the absence of KO<sup>t</sup>Bu base. The decrease of either hydrogen pressure to 5 bar or reaction temperature to 24 °C required 16 hours to obtain 2,2,2-trifluoroethyl alcohol in 91 and 94% yields respectively. A screening study performed by the authors established the following sequence for the efficiency of the base promoters: NaOMe > NaOEt > NaO<sup>t</sup>Pr > KO<sup>t</sup>Bu > KH > KOH. Ethereal solvents (e.g. 1,4-dioxane, THF) afforded the highest catalytic performance while toluene resulted in a lower product yields and the use of methanol led to catalyst deactivation. Eventually, several aliphatic, aromatic or unsaturated fluorinated esters

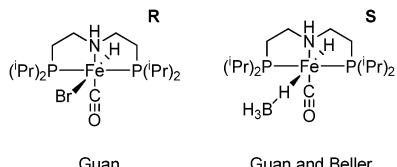
Scheme 31 Milstein's Fe-PNP<sup>197</sup> catalyst for hydrogenation of activated esters.

were hydrogenated using 1%<sub>mol</sub> **Q** (S/C = 100) in combination with 5%<sub>mol</sub> NaOMe at 40 °C and 25 bar H<sub>2</sub>. Moderate yields were generally obtained within 16 hours reaction time. Good chemoselectivity with preservation of functional groups such as ethers, aryl groups, internal and terminal C=C bonds was also demonstrated.

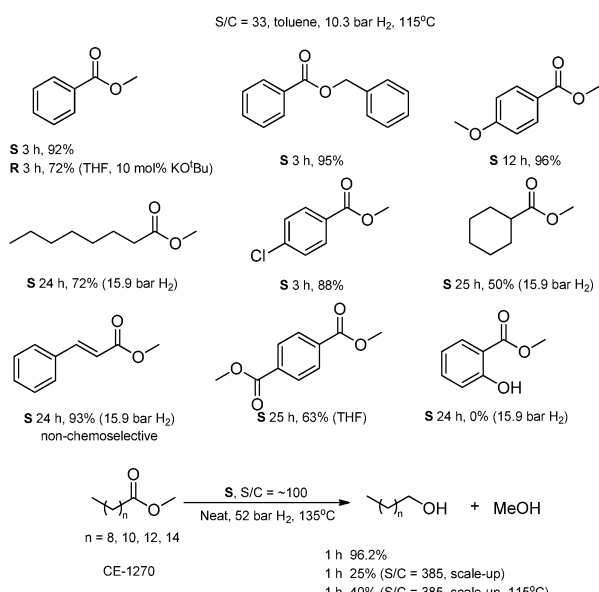
Shortly after the report by Milstein and co-workers, two amino pincer catalysts for hydrogenation of non-activated esters were reported by Guan and co-workers (Scheme 32).<sup>198</sup> Iron complexes **R** and **S** used by Guan and co-workers were in fact utilized before by Beller and co-workers in aqueous phase methanol reforming in late 2013.<sup>199</sup>

Guan and co-workers used the hydrogenation of methyl benzoate as a model reaction to find optimal reaction conditions. At 115 °C and 10.3 bar H<sub>2</sub> pressure the best performance was achieved using toluene as a solvent. A quantitative conversion of methylbenzoate was achieved with 3%<sub>mol</sub> loading of **S** in the absence of base promoter. Catalyst **R** was also active, but





Scheme 32 Fe-PNP amino pincer catalyst employed by Beller<sup>200</sup> and Guan.<sup>198</sup>



Scheme 33 Results of Fe-catalyzed ester hydrogenation reported by Guan.<sup>198</sup>

only in the presence of 10%<sub>mol</sub> KO<sup>t</sup>Bu additive. Therefore, the reactions with **R** resulting in a 72% yield of benzyl alcohol were carried out in THF in order to dissolve the KO<sup>t</sup>Bu base.

Fe-complex **S** was further employed in a substrate screening study (Scheme 33) that included several aromatic and aliphatic esters. Significantly higher hydrogen pressures and longer reaction times were necessary for the hydrogenation of aliphatic esters. The hydrogenation tolerated methoxy- and chlorosubstituents but showed no chemoselectivity in the hydrogenation of methyl cinnamate, leading to formation of 3-phenyl propanol. No activity in hydrogenation of methyl salicylate was observed. The authors further evaluated the activity of **S** in the hydrogenation of fatty acid esters. Reduction of CE-1270, an industrial sample comprised of methyl laurate (C<sub>12</sub>, 73%), methyl myristate (C<sub>14</sub>, 26%) and 1% of C<sub>10</sub> and C<sub>16</sub> esters led to near quantitative yields of the respective alcohols at 135 °C and 52 bar H<sub>2</sub> pressure. Substantial catalyst degradation was already observed after one hour in the scale-up reaction. This effect was, however, minimized by lowering the reaction temperature to 115 °C. The initial rate (TOF°) of CE-1270 reduction was estimated at 137 h<sup>-1</sup>.

Simultaneously with Guan, the group of Beller reported the use of **S** in ester hydrogenation. Noteworthy, this catalyst was reported by the same group as an active nitrile hydrogenation catalyst.<sup>201</sup> At 1%<sub>mol</sub> loading **S** was efficient at 100 °C under

50 bar H<sub>2</sub>. It allowed obtaining a 93% yield of benzyl alcohol within 6 hours reaction time. Similar to the report by Guan, no base additive was required to promote the hydrogenation reaction. Despite **S** requiring no base additive, a comparative base screening study was performed. Surprisingly, the best performance was obtained when no external base was present, with lower yields obtained in the presences of 10%<sub>mol</sub> of KO<sup>t</sup>Bu or Na<sub>2</sub>CO<sub>3</sub>. No conversion was observed in the presence of lithium chloride, methyl sulfonic acid or carbon monoxide. An exceptionally large substrate scope for **S** included aliphatic and aromatic esters, lactones and functionalized substrates (Scheme 34). Good yields were obtained for esters containing O, N, S heterocycles and nitrile groups. In one instance, a chemoselectivity towards ester hydrogenation was demonstrated for esters containing an internal C=C bond.

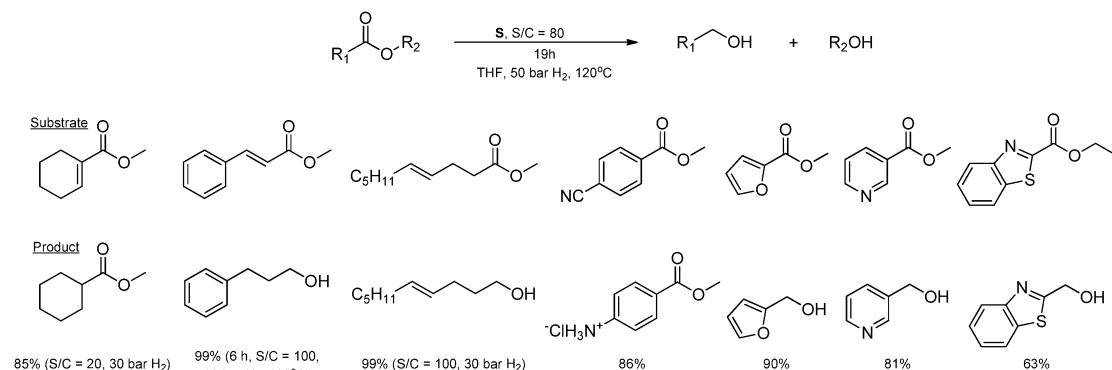
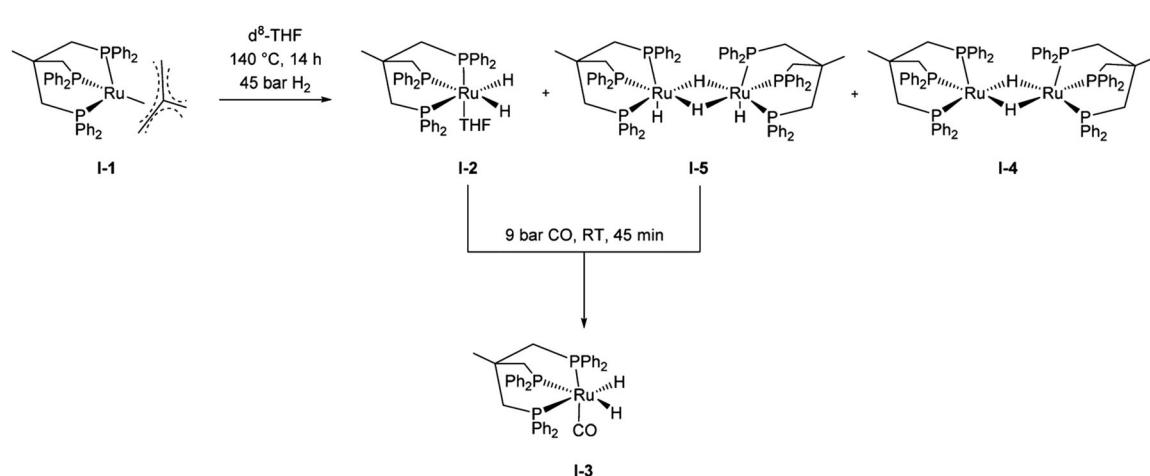
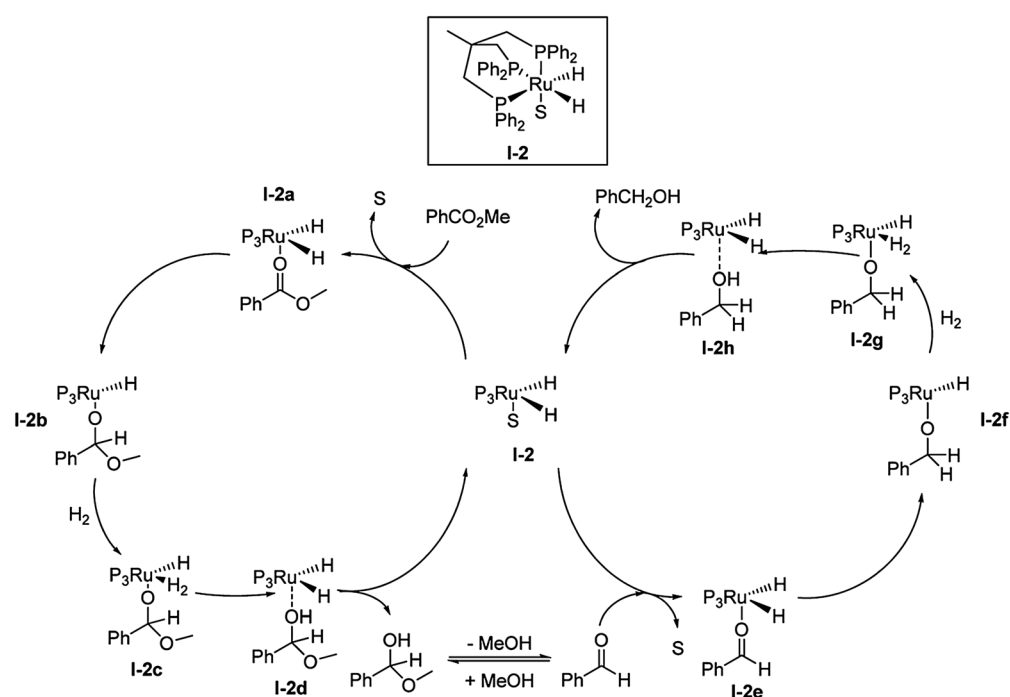
#### 4.4 Mechanisms of ester hydrogenation by homogeneous catalysts

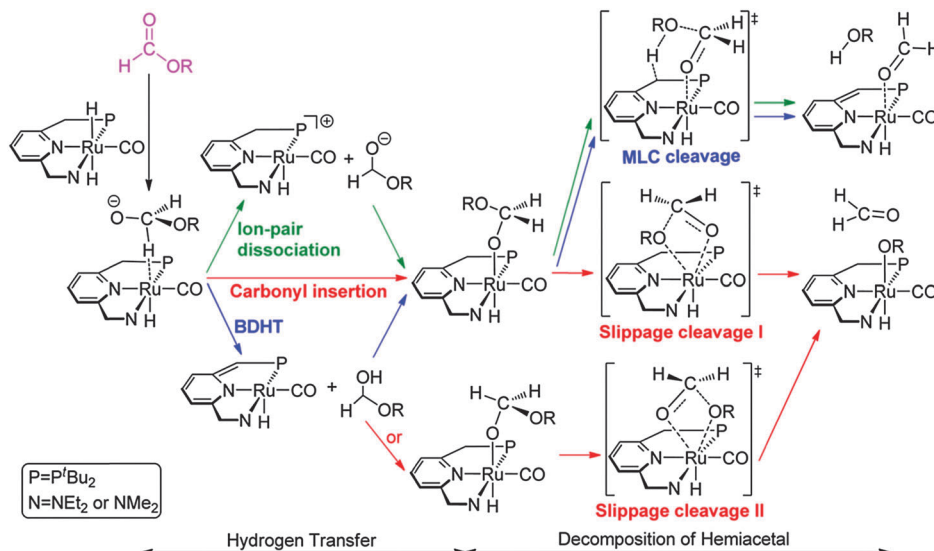
In the final part of the homogeneous catalysis section of this review we will summarize recent mechanistic findings regarding ester hydrogenation reaction. Three typical classes of ester hydrogenation catalysts – TriPhos system, Milstein's Ru-PNN and Ru and Fe amino pincers were studied in detail. Leitner and co-workers<sup>202,203</sup> published a series of works addressing the reactivity of the TriPhos system. Authors found that activation of precatalyst **I-1** (Scheme 35) leads to a set of neutral Ru(II) complexes **I-2** and **I-5** and an Ru(I) dimer **I-4** that were described as being the major source of catalyst deactivation. In addition, deactivation of Ru(II) species by carbonylation was demonstrated experimentally (**I-2(5)** → **I-3**). Interestingly, authors found that addition of catalytic amounts of acid avoids formation or reactivation of the carbonylated species **I-3**. Based on this finding, catalyst deactivation *via* a carbonylation route known to hamper the catalytic performance in reduction of carbonates, ureas and primary amides could be prevented.

A detailed mechanism was also proposed for the hydrogenation of methyl benzoate (Scheme 36), with the reaction proceeding *via* formation of a hemiacetal product, resulting from a hydride insertion into the C=O bond of the substrate (**I-2a** → **I-2b**, Scheme 34) and subsequent hydrogenolysis of Ru–O bond (**I-2c** → **I-2d**, Scheme 36). The latter step was found to be rate determining. The hemiacetal product further undergoes C–O bond cleavage to produce methanol and benzaldehyde, which is subsequently hydrogenated *via* a similar sequence of steps. This mechanism shares a set of similar features with the one proposed by Li and co-workers<sup>83</sup> for ester hydrogenation using a heterogeneous Ru/ZrO<sub>2</sub> catalyst. The hydrogen activation step in both cases is proposed to proceed *via* the formation of σ-H<sub>2</sub>-Ru complex with subsequent heterolytic cleavage of H<sub>2</sub> molecule assisted by the basic site in immediate vicinity to the metal. In case of the TriPhos catalyst the role of the basic site is taken by an alkoxide group of hemiacetal intermediate, while in the case of Ru/ZrO<sub>2</sub> the latter is done by the water molecule or the alkoxy group of the starting ester.

Milstein's Ru-PNN catalyst was by far the most thoroughly investigated system. Scheme 37 represents the summary of



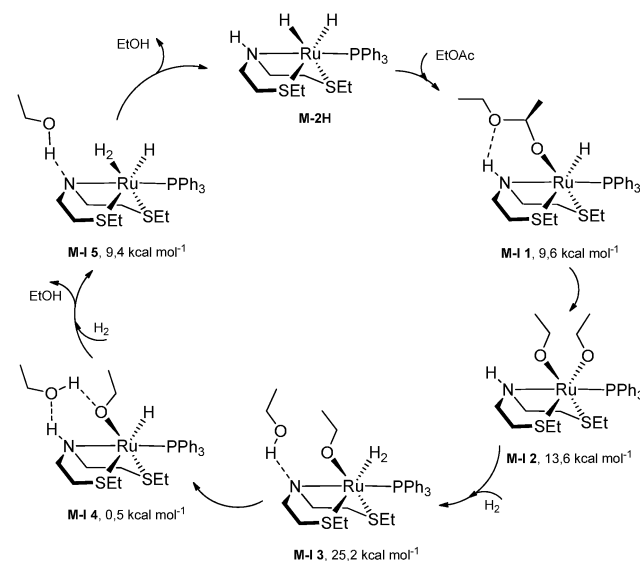
Scheme 34 Substrate scope of Fe-catalysed ester hydrogenation reported by Beller.<sup>201</sup>Scheme 35 Activation of TriPhos catalyst reported by Leitner and co-workers. Reproduced from vom Stein *et al.*, *J. Am. Chem. Soc.*, 2014, **136**, 13217 (ref. 203) by permission of the American Chemical Society.Scheme 36 Mechanism of methyl benzoate hydrogenation by Ru-TriPhos catalyst reported by Leitner and co-workers. Reproduced from vom Stein *et al.*, *J. Am. Chem. Soc.*, 2014, **136**, 13217 (ref. 203) by permission of the American Chemical Society.



Scheme 37 Mechanisms of methyl formate hydrogenation reported by Yang, Hasanayn and Wang summarized by Guan and co-workers.<sup>204</sup> Reproduced from Qu et al., ACS Catal., 2014, **4**, 4377 (ref. 204) by permission of the American Chemical Society.

mechanisms of methyl formate hydrogenation reported by Yang (Green Path),<sup>205</sup> Hasanayn (Red Path)<sup>206</sup> and Wang (Blue Path).<sup>207</sup> The reaction typically proceeds *via* a generation of hemiacetal intermediate and different mechanisms for this step were proposed. Yang<sup>205</sup> outlined the formation of hemiacetal *via* an ion-pair dissociation and subsequent re-coordination of the alkoxy intermediate to Ru complex. Hasanayn<sup>206</sup> reported this step to proceed *via* the carbonyl insertion and finally, Wang<sup>207</sup> proposed a hydride transfer mechanism for direct formation of hemiacetal with concomitant dearomatization of the non-innocent PNP ligand. The decomposition of hemiacetal to produce methanol and corresponding aldehyde was also described by several mechanisms. Hasanayn<sup>206</sup> found a direct hydride/alkoxide metathesis pathway that converts methyl acetate into acetaldehyde and methoxy groups bound to the metal centre. Alternatively, Yang<sup>205</sup> and Wang<sup>207</sup> reported the ligand assisted hemiacetal decomposition. In this mechanism, the non-innocent ligand promotes the C–O cleavage to produce the free alcohol and formaldehyde bound to the metal centre. This pathway was shown to be the most favourable by both groups. The participation of the Lewis-acid Ru site in C–O bond cleavage of hemiacetal intermediate was outlined by Yang,<sup>205</sup> Hasanayn<sup>206</sup> and Wang,<sup>207</sup> although different mechanisms were proposed. On the contrary, Leitner and co-workers proposed the decomposition of hemiacetal to take place outside of the metal coordination sphere for Ru-Triphos-catalysed ester hydrogenation.<sup>203</sup>

State-of-the art Ru-SNS amino pincer catalysts were also subjected to mechanistic analysis by Gusev and co-workers.<sup>191</sup> The authors demonstrated the crucial importance of the NH amine function in catalyst **M**, that suggests the ligand participation in catalysis. Furthermore, they managed to isolate a *cis*-dihydrido Ru-SNS complex (**M-2H**, Scheme 38) as the final catalyst product in acceptorless dehydrogenative coupling of ethanol to ethylacetate and proposed the ester hydrogenation mechanism, based on this intermediate (Scheme 38). In agreement



Scheme 38 Mechanisms of ethyl acetate hydrogenation proposed by Gusev and co-workers.<sup>191</sup>

with proposal by Milstein<sup>173</sup> and Saudan,<sup>185</sup> the first step in the mechanism included the carbonyl insertion into Ru–H bond resulting in a hemiacetal intermediate **M-I 1**. Interestingly, the authors found the stabilization of the hemiacetal intermediate by the cooperative NH group of the ligand *via* the formation of NH···O hydrogen bond. Subsequent internal substitution leads to the bis-(alkoxy) intermediate **M-I 2**. The latter subsequently undergoes hydrogenolysis *via* the intermediate formation of molecular hydrogen complexes to yield the alcohol product. This mechanism is conceptually different as it involves the formation of a bis-(alkoxy) intermediate rather than the stepwise formation of aldehyde intermediates and their subsequent hydrogenation, as was proposed for the Milstein Ru-PNP system.<sup>204,205</sup> In addition, the mechanism proposed by Gusev



outlines the participation of the cooperative NH function in several reaction steps. Being consistent with experimental work by Takebayashi and Bergens,<sup>208</sup> this observation provides an additional support for the bifunctional nature of catalysis in ester hydrogenation.

## 5. Concluding remarks

Over the past two decades, catalysis for the hydrogenation of carboxylic acids and esters has gathered substantial interest. Researchers managed to develop chemoselective reduction protocols in homogeneous<sup>185</sup> and heterogeneous<sup>107,108</sup> processes; the efficiency of homogeneous ester hydrogenation catalysts was increased by nearly three orders of magnitude<sup>194</sup> compared with early examples. Some remarkable progress has also been made in heterogeneous catalysts capable of operating at mild temperatures and pressures (*ca.* 100 °C/20–30 bar H<sub>2</sub>). These conditions represent the current state-of-the-art for fatty acid hydrogenation.

Improvements in the performance of heterogeneous catalysts were based on the recognition of the importance of metal–metal and metal–support synergy. The bifunctional character is therefore generally accepted for ester hydrogenation catalysis. Such bifunctional ensembles can be formed in several different ways. First examples include bimetallic catalysts in which one metal facilitates heterolytic H<sub>2</sub> cleavage and hydrogenation steps, while the second metal activates the carbonyl group of the acid/ester molecule. Catalysts combining hydrogenation (*e.g.* Ru, Pt, Pd) and promoter (*e.g.* Sn, Re, Mo) metals show substantial synergy. In addition, support materials such as TiO<sub>2</sub> and ZnO may assist in carbonyl group and/or dihydrogen activation. Thus, cooperativity between Lewis or Brønsted acid sites and metal hydrogenation function appears to be particularly important. Finally, other components of the reaction medium such as, for example, a water solvent, may also facilitate bifunctional hydrogenation mechanisms over oxide supported catalysts.

Similar to the heterogeneous catalysts, the vast majority of homogeneous ester hydrogenation catalysts are in fact bifunctional in nature. Acid–base non-innocent ligands provide the cooperative function in homogeneous transition metal catalysts. Particularly, Noyori–Ikariya type bifunctional catalysts, based on polydentate amino-ligands, comprise the current state of the art. The application of amino pincer ligand platform currently spans beyond Ru-based ester hydrogenation. As demonstrated in several reports in 2014, the use of PNP amino pincers can induce the activity of otherwise inactive metals, *e.g.* iridium<sup>209</sup> and iron. The replacement of noble metals in homogeneous ester hydrogenation catalysts can be viewed as the most significant recent achievement in the field, which will likely fuel new research activities.

Two major problems may be mentioned relevant to ester hydrogenation. The first one is the lack of adequate comparison between different catalysts. Considering that the substrate scope and testing conditions vary significantly across the literature, the accurate comparison of different catalysts is not trivial. Secondly, the activity data is typically presented in terms

of TON values or product yields, which are crucial from the application point of view, but provide very little insight into the intrinsic activity of the catalyst. This problem can be partially resolved by kinetic studies, where initial hydrogenation rates can be determined. Both aspects have only been addressed to a limited extent so far and invite for follow-up work.

Finally, we stress the importance of resolving the mechanism of carboxylic acid and ester hydrogenation. Homogeneous and heterogeneous catalysts have been applied extensively using complementary experimental techniques. In addition, well-defined homogeneous systems were also subject to rather comprehensive DFT studies. We believe that further development of a molecular understanding of catalytic action of multi-component homogeneous and heterogeneous systems can ultimately bring together these fields. Given the intriguing similarity of mechanistic proposals put forward for these very different classes, the development of a unified model describing the reduction of carboxylic acid derivatives seems realistic. Such a uniform conceptual description of the reaction mechanism would create a basis for a rational design of new and improved catalysts.

## Acknowledgements

This work has been partially performed within the framework of the CatchBio program. The authors gratefully acknowledge the support of the Smart Mix Program of the Netherlands Ministry of Economic Affairs and the Netherlands Ministry of Education, Culture and Science. E.A.P. thanks the Technology Foundation STW and the Netherlands Organization for Scientific Research (NWO) for his personal VENI grant.

## Notes and references

- 1 A. Corma, S. Iborra and A. Velty, *Chem. Rev.*, 2007, **107**, 2411–2502.
- 2 T. Voeste and H. Buchold, *J. Am. Oil Chem. Soc.*, 1984, **61**, 350–352.
- 3 A. Behr, A. Westfechtel and J. Perez Gomes, *Chem. Eng. Technol.*, 2008, **31**, 700–714.
- 4 B. Chen, U. Dingerdissen, J. G. E. Krauter, H. G. J. Lansink Rotgerink, K. Moebus, D. J. Ostgard, P. Panster, T. H. Riermeier, S. Seebald, T. Tacke and H. Trauthwein, *Appl. Catal., A*, 2005, **280**, 17–46.
- 5 H. Mimoun, G. Holzner and J. Pastori, *US Pat.*, 6,806,250, 2014.
- 6 M. Eini and D. Tamarkin, *US Pat.*, 6,994,863, 2006.
- 7 J. U. Kaw and L. B. Steuri, *US Pat.*, 5,089,174, 1992.
- 8 B. D. Buddemeyer, M. S. Fish, D. P. Leonard and H. H. Miers, *US Pat.*, 3,623,887, 1971.
- 9 G. L. Castiglioni, M. Ferrari, A. Guercio, A. Vaccari, R. Lancia and C. Fumagalli, *Catal. Today*, 1996, **27**, 181–186.
- 10 J. Martinussen, C. Solem, A. K. Holm and P. R. Jensen, *Curr. Opin. Chem. Biol.*, 2013, **24**, 124–129.
- 11 J. Kuiper, *US Pat.*, 4,278,609, 1979.



12 G. M. Qualeatti and B. J. Arena, *US Pat.*, 4,519,951, 1985.

13 B. Flach, K. Bendz, S. Lieberz, *EU Biofuels Annual*, 2014, US Depatrment of Agriculture Report, 2014.

14 B. Zhang, S. Hui, S. Zhang, Y. Ji, W. Li and D. Fang, *J. Nat. Gas Chem.*, 2012, **21**, 563–570.

15 Z. He, H. Lin, P. He and Y. Yuan, *J. Catal.*, 2011, **277**, 54–63.

16 J. Zheng, H. Lin, X. Zheng, X. Duan and Y. Yuan, *Catal. Commun.*, 2013, **40**, 129–133.

17 A. Yin, X. Guo, K. Fan and W.-L. Dai, *ChemCatChem*, 2010, **2**, 206–213.

18 T. Turek, D. L. Trimm and N. W. Cant, *Catal. Rev.: Sci. Eng.*, 1994, **36**, 645–683.

19 P. A. Dub and T. Ikariya, *ACS Catal.*, 2012, **2**, 1718–1741.

20 A. M. Smith and R. Whyman, *Chem. Rev.*, 2014, **114**, 5477–5510.

21 C. Maeda, Y. Miyazaki and T. Ema, *Catal. Sci. Technol.*, 2014, **4**, 1482–1497.

22 Y.-N. Li, R. Ma, L.-N. He and Z.-F. Diao, *Catal. Sci. Technol.*, 2014, **4**, 1498–1512.

23 G. A. Olah, *Angew. Chem., Int. Ed.*, 2005, **44**, 2636–2639.

24 C. A. Huff and M. S. Sanford, *J. Am. Chem. Soc.*, 2011, **133**, 18122–18125.

25 E. Balaraman, C. Gunanathan, J. Zhang, L. J. W. Shimon and D. Milstein, *Nat. Chem.*, 2011, **3**, 609–614.

26 T. van Haasterecht, T. W. van Deelen, K. P. de Jong and J. H. Bitter, *Catal. Sci. Technol.*, 2014, **4**, 2353–2366.

27 G. Zeng, S. Sakaki, K.-I. Fujita, H. Sano and R. Yamaguchi, *ACS Catal.*, 2014, **4**, 1010–1020.

28 P. Liu and E. J. M. Hensen, *J. Am. Chem. Soc.*, 2013, **135**, 14032–14035.

29 D. I. Enache, J. K. Edwards, P. Landon, B. Solsona-Espriu, A. F. Carley, A. A. Herzing, M. Watanabe, C. J. Kiely, D. W. Knight and G. J. Hutchings, *Science*, 2006, **311**, 362–365.

30 Y. Zhang, C.-S. Lim, D. S. B. Sim, H.-J. Pan and Y. Zhao, *Angew. Chem., Int. Ed.*, 2014, **53**, 1399–1403.

31 C. Gunanathan and D. Milstein, *Acc. Chem. Res.*, 2011, **44**, 588–602.

32 C. Gunanathan and D. Milstein, *Science*, 2013, **341**, 249.

33 B. Gnanaprakasam, J. Zhang and D. Milstein, *Angew. Chem., Int. Ed.*, 2010, **49**, 1468–1471.

34 L. Bouveault and G. Blanc, *Compt. Rend.*, 1903, **136**, 1676–1678.

35 J. J. Li, *Name Reactions: A Collection of Detailed Mechanisms and Synthetic Applications*, Springer, 3rd edn, 2007.

36 B. S. Bodnar and P. F. Vogt, *J. Org. Chem.*, 2009, **74**, 2598–2600.

37 P. Urben, *Bretherick's Handbook of Reactive Chemical Hazards*, Academic Press, 6th edn, 2006.

38 J. Clayden, N. Greeves, S. Warren and P. Wothers, *Organic Chemistry*, Oxford University Press, 2000.

39 H. Adkins and R. Connor, *J. Am. Chem. Soc.*, 1931, **53**, 1091–1095.

40 M. Ahmadi, E. E. Macias, J. B. Jasinski, P. Ratnasamy and M. A. Carreon, *J. Mol. Catal. A: Chem.*, 2014, **386**, 14–19.

41 K. Kon, W. Onodera, S. Takakusagi and K.-I. Shimizu, *Catal. Sci. Technol.*, 2014, **4**, 3705–3712.

42 H. F. Rase, *Handbook of Commercial Catalysts: Heterogeneous Catalysts*, CRC Press, 1st edn, 2000.

43 H. I. Adkins and A. A. Pavlic, *J. Am. Chem. Soc.*, 1947, **69**, 3039–3041.

44 H. Adkins and K. Folkers, *J. Am. Chem. Soc.*, 1931, **53**, 1095–1097.

45 H. Adkins, H. I. Cramer and R. Connor, *J. Am. Chem. Soc.*, 1931, **53**, 1402–1405.

46 R. Connor, K. Folkers and H. Adkins, *J. Am. Chem. Soc.*, 1932, **54**, 1138–1145.

47 K. Folkers and H. Adkins, *J. Am. Chem. Soc.*, 1932, **54**, 1145–1154.

48 H. Adkins, B. Wojcik and L. W. Covert, *J. Am. Chem. Soc.*, 1933, **55**, 1669–1676.

49 U. R. Kreutzer, *J. Am. Oil Chem. Soc.*, 1984, **61**, 343–348.

50 D. S. Thakur, B. D. Roberts, T. J. Sullivan and A. L. Vichek, *US Pat.*, 5,155,086, 1992.

51 Y. Hattori, K. Yamamoto, J. Kaita, M. Matsuda and S. Yamada, *J. Am. Oil Chem. Soc.*, 2000, **77**, 1283–1287.

52 B. Bender, M. Berweiler, K. Moebus, D. Ostgard and G. Stein, *US Pat.*, 6,489,521, 2002.

53 R. Fischer, R. Pinkos and F. Stein, *US Pat.*, 6,426,438, 2002.

54 H. Hirayama, *Jp. Pat.*, 07206737, 1995.

55 Y. Ishimura, H. Hirayama, T. Nozawa and H. Monzen, *Jp. Pat.*, 09059188, 1997.

56 J. W. Evans, M. S. Wainwright, N. W. Cant and D. L. Trimm, *J. Catal.*, 1984, **88**, 203–213.

57 A. K. Agarwal, N. W. Cant, M. S. Wainwright and D. L. Trimm, *J. Mol. Catal.*, 1987, **43**, 79–92.

58 A. K. Agarwal, M. S. Wainwright, D. L. Trimm and N. W. Cant, *J. Mol. Catal.*, 1988, **45**, 247–254.

59 T. Turek, D. L. Trimm, D. S. Black and N. W. Cant, *Appl. Catal., A*, 1994, **116**, 137–150.

60 D. S. Brands, E. K. Poels, T. A. Krieger, O. V. Makarova, C. Weber, S. Veer and A. Bliek, *Catal. Lett.*, 1996, **36**, 175–181.

61 D. S. Brands, E. K. Poels and A. Bliek, *Appl. Catal., A*, 1999, **184**, 279–289.

62 E. K. Poels and D. S. Brands, *Appl. Catal., A*, 2000, **191**, 83–96.

63 K. C. Waugh, *Catal. Today*, 1993, **18**, 147–162.

64 G. Vedage and K. Klier, *J. Catal.*, 1982, **77**, 558–560.

65 D. S. Brands, G. Sai, E. K. Poels and A. Bliek, *J. Catal.*, 1999, **186**, 169–180.

66 H. Huang, G. Cao and S. Wang, *J. Ind. Eng. Chem.*, 2014, **20**, 988–993.

67 H. Huang, G. Cao and S. Wang, *Korean J. Chem. Eng.*, 2013, **30**, 1710–1715.

68 Y. Pouilloux, F. Autin and J. Barrault, *Catal. Today*, 2000, **63**, 87–100.

69 H. Huang, S. Wang, S. Wang and G. Cao, *Catal. Lett.*, 2010, **134**, 351–357.

70 H. Huang, G. Cao, C. Fan, S. Wang and S. Wang, *Korean J. Chem. Eng.*, 2009, **26**, 1574–1579.

71 B. E. Green, C. S. Sass, L. T. Germinario, P. S. Wehner and B. L. Gustafson, *J. Catal.*, 1993, **140**, 406–417.



72 C. Hu, D. Creaser, S. Siahrostami, H. Groenbeck, H. Ojagh and M. Skoglundh, *Catal. Sci. Technol.*, 2014, **4**, 2427–2444.

73 V. M. Deshpande, W. R. Patterson and C. S. Narasimhan, *J. Catal.*, 1990, **121**, 165–173.

74 V. M. Deshpande, K. Ramnarayan and C. S. Narasimhan, *J. Catal.*, 1990, **121**, 174–182.

75 Y. Pouilloux, F. Autin, C. Guimon and J. Barrault, *J. Catal.*, 1998, **176**, 215–224.

76 D. A. Echeverri, J. M. Marin, G. M. Restrepo and L. A. Rios, *Appl. Catal., A*, 2009, **366**, 342–347.

77 T. Miyake, T. Makino, S.-I. Taniguchi, H. Watanuki, T. Niki, S. Shimizu, Y. Kojima and M. Sano, *Appl. Catal., A*, 2009, **364**, 108–112.

78 Y. Pouilloux, A. Piccirilli and J. Barrault, *J. Mol. Catal. A: Chem.*, 1996, **108**, 161–166.

79 Y. Pouilloux, F. Autin, A. Piccirilli, C. Guimon and J. Barrault, *Appl. Catal., A*, 1998, **169**, 65–75.

80 K. De Oliveira, Y. Pouilloux and J. Barrault, *J. Catal.*, 2001, **204**, 230–237.

81 M. A. Sánchez, V. A. Mazzieri, M. Oportus, P. Reyes and C. L. Pieck, *Catal. Today*, 2013, **213**, 81–86.

82 Y. Zhou, H. Fu, X. Zheng, R. Li, H. Chen and X. Li, *Catal. Commun.*, 2009, **11**, 137–141.

83 G. Fan, Y. Zhou, H. Fu, X. Ye, R. Li, H. Chen and X. Li, *Chin. J. Chem.*, 2011, **29**, 229–236.

84 F. C. A. Figueiredo, E. Jordao, R. Landers and W. A. Carvalho, *Appl. Catal., A*, 2009, **371**, 131–141.

85 S. M. dos Santos, A. M. Silva, E. Jordao and M. A. Fraga, *Catal. Today*, 2005, **107–108**, 250–257.

86 S. R. De Miguel, M. C. Roman-Martinez, E. L. Jablonski, J. L. G. Fierro, D. Cazorla-Amoros and O. A. Scelza, *J. Catal.*, 1999, **184**, 514–525.

87 A. Auroux, D. Sprinceana and A. Gervasini, *J. Catal.*, 2000, **195**, 140–150.

88 N. Nava and T. Viveros, *Hyperfine Interact.*, 1999, **122**, 147–153.

89 E. A. Sales, J. Jove, M. d. J. Mendes and F. Bozon-Verduraz, *J. Catal.*, 2000, **195**, 88–95.

90 C. Huang, H. Zhang, Y. Zhao, S. Chen and Z. Liu, *J. Colloid Interface Sci.*, 2012, **386**, 60–65.

91 A. Yin, X. Guo, W.-L. Dai, H. Li and K. Fan, *Appl. Catal., A*, 2008, **349**, 91–99.

92 A. Yin, C. Wen, W.-L. Dai and K. Fan, *Appl. Surf. Sci.*, 2011, **257**, 5844–5849.

93 A. Yin, X. Guo, K. Fan and W.-L. Dai, *Appl. Catal., A*, 2010, **377**, 128–133.

94 H. Lin, X. Zheng, Z. He, J. Zheng, X. Duan and Y. Yuan, *Appl. Catal., A*, 2012, **445–446**, 287–296.

95 Y. Cui, C. Wen, X. Chen and W.-L. Dai, *RSC Adv.*, 2014, **4**, 31162–31165.

96 L.-F. Chen, P.-J. Guo, M.-H. Qiao, S.-R. Yan, H.-X. Li, W. Shen, H.-L. Xu and K.-N. Fan, *J. Catal.*, 2008, **257**, 172–180.

97 J. Zheng, H. Lin, Y.-N. Wang, X. Zheng, X. Duan and Y. Yuan, *J. Catal.*, 2013, **297**, 110–118.

98 Y.-N. Wang, X. Duan, J. Zheng, H. Lin, Y. Yuan, H. Ariga, S. Takakusagi and K. Asakura, *Catal. Sci. Technol.*, 2012, **2**, 1637–1639.

99 Y. Zhu, Y. Zhu, G. Ding, S. Zhu, H. Zheng and Y. Li, *Appl. Catal., A*, 2013, **468**, 296–304.

100 S. H. Jhung, J. W. Yoon, J. S. Lee and J.-S. Chang, *Chem. – Eur. J.*, 2007, **13**, 6502–6507.

101 H. Nakatsuji, Z.-M. Hu, H. Nakai and K. Ikeda, *Surf. Sci.*, 1997, **387**, 328–341.

102 A. Wittstock, V. Zielasek, J. Biener, C. M. Friend and M. Baumer, *Science*, 2010, **327**, 319–322.

103 H. G. Manyar, C. Paun, R. Pilus, D. W. Rooney, J. M. Thompson and C. Hardacre, *Chem. Commun.*, 2010, **46**, 6279–6281.

104 K. S. Kim and M. A. Barteau, *Langmuir*, 1988, **4**, 945–953.

105 D.-H. He, N. Wakasa and T. Fuchikami, *Tetrahedron Lett.*, 1995, **36**, 1059–1062.

106 L. Fabre, P. Gallezot and A. Perrard, *J. Catal.*, 2002, **208**, 247–254.

107 K. Tahara, E. Nagahara, Y. Itoi, S. Nishiyama, S. Tsuruya and M. Masai, *J. Mol. Catal. A: Chem.*, 1996, **110**, L5–L6.

108 K. Tahara, E. Nagahara, Y. Itoi, S. Nishiyama, S. Tsuruya and M. Masai, *Appl. Catal., A*, 1997, **154**, 75–86.

109 M. Toba, S.-I. Tanaka, S.-I. Niwa, F. Mizukami, Z. Koppány, L. Guczi, K.-Y. Cheah and T.-S. Tang, *Appl. Catal., A*, 1999, **189**, 243–250.

110 Y. Hara and K. Endou, *Appl. Catal., A*, 2003, **239**, 181–195.

111 Z. Zhu, Z. Lu, B. Li and S. Guo, *Appl. Catal., A*, 2006, **302**, 208–214.

112 M. A. Sánchez, Y. Pouilloux, V. A. Mazzieri and C. L. Pieck, *Appl. Catal., A*, 2013, **467**, 552–558.

113 M. J. Mendes, O. A. A. Santos, E. Jordão and A. M. Silva, *Appl. Catal., A*, 2001, **217**, 253–262.

114 W. Rachmady and M. A. Vannice, *J. Catal.*, 2000, **192**, 322–334.

115 A. Primo, P. Concepcion and A. Corma, *Chem. Commun.*, 2011, **47**, 3613–3615.

116 L. Chen, Y. Zhu, H. Zheng, C. Zhang and Y. Li, *Appl. Catal., A*, 2012, **411–412**, 95–104.

117 L. Chen, Y. Li, X. Zhang, Q. Zhang, T. Wang and L. Ma, *Appl. Catal., A*, 2014, **478**, 117–128.

118 L. Chen, Y. Zhu, H. Zheng, C. Zhang, B. Zhang and Y. Li, *J. Mol. Catal. A: Chem.*, 2011, **351**, 217–227.

119 H. S. Broadbent and C. W. Whittle, *J. Am. Chem. Soc.*, 1959, **81**, 3587–3589.

120 H. S. Broadbent, G. C. Campbell, W. J. Bartley and J. H. Johnson, *J. Org. Chem.*, 1959, **24**, 1847–1854.

121 R. E. Bockrath, D. Campos, J.-A. T. Schwartz, C. Ford and R. T. Stimek, *US Pat.*, 6,008,384, 1999.

122 D. Campos, R. E. Ernst and J. B. Michel, *US Pat.*, 6,566,539, 2003.

123 R. V. Chaudhari, C. V. Rode, R. M. Deshpande, R. Jaganathan, T. M. Leib and P. L. Mills, *Chem. Eng. Sci.*, 2003, **58**, 627–632.

124 B. K. Ly, D. P. Minh, C. Pinel, M. Besson, B. Tapin, F. Epron and C. Espezel, *Top. Catal.*, 2012, **55**, 466–473.

125 C. Bolivar, H. Charcosset, R. Frety, M. Primet, L. Tournayan, C. Betizeau, G. Leclercq and R. Maurel, *J. Catal.*, 1975, **39**, 249–259.



126 C. Betizeau, G. Leclercq, R. Maurel, C. Bolivar, H. Charcosset, R. Frety and L. Tournayan, *J. Catal.*, 1976, **45**, 179–188.

127 A. Ciftci, D. A. J. M. Ligthart, A. O. Sen, A. J. F. van Hoof, H. Friedrich and E. J. M. Hensen, *J. Catal.*, 2014, **311**, 88–101.

128 A. Ciftci, D. A. J. M. Ligthart and E. J. M. Hensen, *Green Chem.*, 2014, **16**, 853–863.

129 C. Delhomme, D. Weuster-Botz and F. E. Kuehn, *Green Chem.*, 2009, **11**, 13–26.

130 D. P. Minh, M. Besson, C. Pinel, P. Fuertes and C. Petitjean, *Top. Catal.*, 2010, **53**, 1270–1273.

131 M. Chia, Y. J. Pagan-Torres, D. Hibbitts, Q.-H. Tan, H. N. Pham, A. K. Datye, M. Neurock, R. J. Davis and J. A. Dumesic, *J. Am. Chem. Soc.*, 2011, **133**, 12675–12689.

132 Y. Takeda, Y. Nakagawa and K. Tomishige, *Catal. Sci. Technol.*, 2012, **2**, 2221–2223.

133 J. Sa, C. Kartusch, M. Makosch, C. Paun, J. A. van Bokhoven, E. Kleymenov, J. Szlachetko, M. Nachtegaal, H. G. Manyar and C. Hardacre, *Chem. Commun.*, 2011, **47**, 6590–6592.

134 M. Stein and B. Breit, *Angew. Chem., Int. Ed.*, 2013, **52**, 2231–2234.

135 R. Burch, C. Paun, X. M. Cao, P. Crawford, P. Goodrich, C. Hardacre, P. Hu, L. McLaughlin, J. Sa and J. M. Thompson, *J. Catal.*, 2011, **283**, 89–97.

136 J. Coetzee, H. G. Manyar, C. Hardacre and D. J. Cole-Hamilton, *ChemCatChem*, 2013, **5**, 2843–2847.

137 S. Werkmeister, K. Junge and M. Beller, *Org. Process Res. Dev.*, 2014, **18**, 289–302.

138 R. Luque and J. H. Clark, *Catal. Commun.*, 2010, **11**, 928–931.

139 Z. Zhang, J. E. Jackson and D. J. Miller, *Appl. Catal., A*, 2001, **219**, 89–98.

140 Y. Takeda, T. Shoji, H. Watanabe, M. Tamura, Y. Nakagawa, K. Okumura and K. Tomishige, *ChemSusChem*, 2015, **8**, 1170–1178.

141 S. Koso, H. Watanabe, K. Okumura, Y. Nakagawa and K. Tomishige, *Appl. Catal., B*, 2012, **111–112**, 27–37.

142 Z. Wang, G. Li, X. Liu, Y. Huang, A. Wang, W. Chu, X. Wang and N. Li, *Catal. Commun.*, 2014, **43**, 38–41.

143 P. Mäki-Arvela, I. L. Simakova, T. Salmi and D. Y. Murzin, *Chem. Rev.*, 2013, **114**, 1909–1971.

144 A. M. R. Galletti, C. Antonetti, V. De Luise and M. Martinelli, *Green Chem.*, 2012, **14**, 688–694.

145 A. M. R. Galletti, C. Antonetti, E. Ribechini, M. P. Colombini, N. Nassio Di Nasso and E. Bonari, *Appl. Energy*, 2013, **102**, 157–162.

146 O. A. Abdelrahman, A. Heyden and J. Q. Bond, *ACS Catal.*, 2014, **4**, 1171–1181.

147 M. Chalid, H. J. Heeres and A. A. Broekhuis, *Procedia Chem.*, 2012, **4**, 260–267.

148 A. Demolis, N. Essayem and F. Rataboul, *ACS Sustainable Chem. Eng.*, 2014, **2**, 1338–1352.

149 W. Luo, M. Sankar, A. M. Beale, Q. He, C. J. Kiely, P. C. A. Bruijninx and B. M. Weckhuysen, *Nat. Commun.*, 2015, **6**, 6540.

150 V. Mohan, V. Venkateshwarlu, C. V. Pramod, B. D. Raju and K. S. R. Rao, *Catal. Sci. Technol.*, 2014, **4**, 1253–1259.

151 V. Mohan, C. Raghavendra, C. V. Pramod, B. D. Raju and K. S. Rama Rao, *RSC Adv.*, 2014, **4**, 9660–9668.

152 M. Besson, P. Gallezot and C. Pinel, *Chem. Rev.*, 2013, **114**, 1827–1870.

153 M. Li, G. Li, N. Li, A. Wang, W. Dong, X. Wang and Y. Cong, *Chem. Commun.*, 2014, **50**, 1414–1416.

154 L. Corbel-Demilly, B.-K. Ly, D.-P. Minh, B. Tapin, C. Espezel, F. Epron, A. Cabiac, E. Guillon, M. Besson and C. Pinel, *ChemSusChem*, 2013, **6**, 2388–2395.

155 X.-L. Du, Q.-Y. Bi, Y.-M. Liu, Y. Cao, H.-Y. He and K.-N. Fan, *Green Chem.*, 2012, **14**, 935–939.

156 R. V. Christian Jr, H. D. Brown and R. M. Hixon, *J. Am. Chem. Soc.*, 1947, **69**, 1961–1963.

157 J. M. Bermudez, J. A. Menendez, A. A. Romero, E. Serrano, J. Garcia-Martinez and R. Luque, *Green Chem.*, 2013, **15**, 2786–2792.

158 E. Balaraman and D. Milstein, *Top. Organomet. Chem.*, Springer, Berlin Heidelberg, 2014, vol. 77, pp. 1–25.

159 C. Gunanathan and D. Milstein, *Chem. Rev.*, 2014, **114**, 12024–12087.

160 R. A. Grey, G. P. Pez, A. Wallo and J. Corsi, *Chem. Commun.*, 1980, 783–784.

161 G. P. Pez, R. A. Grey and J. Corsi, *J. Am. Chem. Soc.*, 1981, **103**, 7528–7535.

162 R. A. Grey, G. P. Pez and A. Wallo, *J. Am. Chem. Soc.*, 1981, **103**, 7536–7542.

163 U. Matteoli, G. Menchi, M. Bianchi and F. Piacenti, *J. Organomet. Chem.*, 1986, **299**, 233–238.

164 Y. Kara and K. Wada, *Chem. Lett.*, 1991, 553–554.

165 Y. Hara, H. Inagaki, S. Nishimura and K. Wada, *Chem. Lett.*, 1992, 1983–1986.

166 H. T. Teunissen and C. J. Elsevier, *Chem. Commun.*, 1997, 667–668.

167 H. T. Teunissen, *Chem. Commun.*, 1998, 1367–1368.

168 U. Matteoli, M. Bianchi, G. Menchi, P. Prediani and F. Piacenti, *J. Mol. Catal.*, 1984, **22**, 353–362.

169 L. Rosi, M. Frediani and P. Frediani, *J. Organomet. Chem.*, 2010, **695**, 1314–1322.

170 M. J. Hanton, S. Tin, B. J. Boardman and P. Miller, *J. Mol. Catal. A: Chem.*, 2011, **346**, 70–78.

171 M. C. van Engelen, H. T. Teunissen, J. G. de Vries and C. J. Elsevier, *J. Mol. Catal. A: Chem.*, 2003, **206**, 185–192.

172 F. M. A. Geilen, B. Engendahl, A. Harwardt, W. Marquardt, J. Klankermayer and W. Leitner, *Angew. Chem., Int. Ed.*, 2010, **49**, 5510–5514.

173 J. Zhang, G. Leitus, Y. Ben-David and D. Milstein, *Angew. Chem., Int. Ed.*, 2006, **45**, 1113–1115.

174 C. Gunanathan and D. Milstein, *Acc. Chem. Res.*, 2011, **44**, 588–602.

175 E. Fogler, E. Balaraman, Y. Ben-David, G. Leitus, L. J. W. Shimon and D. Milstein, *Organometallics*, 2011, **30**, 3826–3833.

176 Y. Sun, C. Koehler, R. Tan, V. T. Annibale and D. Song, *Chem. Commun.*, 2011, **47**, 8349–8351.



177 G. A. Filonenko, E. Cosimi, L. Lefort, M. P. Conley, C. Coperet, M. Lutz, E. J. M. Hensen and E. A. Pidko, *ACS Catal.*, 2014, **4**, 2667–2671.

178 R. Noyori, *Angew. Chem., Int. Ed.*, 2002, **41**, 2008–2022.

179 K. Abdur-Rashid, S. E. Clapham, A. Hadzovic, J. N. Harvey, A. J. Lough and R. H. Morris, *J. Am. Chem. Soc.*, 2002, **124**, 15104–15118.

180 K. Abdur-Rashid, R. Guo, A. J. Lough, R. H. Morris and D. Song, *Adv. Synth. Catal.*, 2005, **347**, 571–579.

181 T. Ikariya, K. Murata and R. Noyori, *Org. Biomol. Chem.*, 2006, **4**, 393–406.

182 J.-X. Gao, H. Zhang, X.-D. Yi, P.-P. Xu, C.-L. Tang, H.-L. Wan, K.-R. Tsai and T. Ikariya, *Chirality*, 2000, **12**, 383–388.

183 J. S. M. Samec, J.-E. Backvall, P. G. Andersson and P. Brandt, *Chem. Soc. Rev.*, 2006, **35**, 237–248.

184 S. Gladiali and E. Alberico, *Chem. Soc. Rev.*, 2006, **35**, 226–236.

185 L. A. Saudan, C. M. Saudan, C. Debieux and P. Wyss, *Angew. Chem., Int. Ed.*, 2007, **46**, 7473–7476.

186 I. Carpenter, S. C. Eckelmann, M. T. Kuntz, J. A. Fuentes, M. B. France and M. L. Clarke, *Dalton Trans.*, 2012, **41**, 10136–10140.

187 P. Maire, T. Büttner, F. Breher, P. Le Floch and H. Grützmacher, *Angew. Chem., Int. Ed.*, 2005, **44**, 6318–6323.

188 A. Friedrich, M. Drees, M. Käss, E. Herdtweck and S. Schneider, *Inorg. Chem.*, 2010, **49**, 5482–5494.

189 W. Kuriyama, T. Matsumoto, O. Ogata, Y. Ino, K. Aoki, S. Tanaka, K. Ishida, T. Kobayashi, N. Sayo and T. Saito, *Org. Process Res. Dev.*, 2011, **16**, 166–171.

190 D. Spasyuk, S. Smith and D. G. Gusev, *Angew. Chem., Int. Ed.*, 2012, **51**, 2772–2775.

191 D. Spasyuk, S. Smith and D. G. Gusev, *Angew. Chem., Int. Ed.*, 2013, **52**, 2538–2542.

192 D. Goussev, D. Spasyuk and S. Smith, *WO Pat.*, 2014036650, 2014.

193 D. Spasyuk, C. Vicent and D. G. Gusev, *J. Am. Chem. Soc.*, 2015, **137**, 3743–3746.

194 W. Li, J.-H. Xie, M.-L. Yuan and Q.-L. Zhou, *Green Chem.*, 2014, **16**, 4081–4085.

195 X. Tan, Y. Wang, Y. Liu, F. Wang, L. Shi, K.-H. Lee, Z. Lin, H. Lv and X. Zhang, *Org. Lett.*, 2015, **17**, 454–457.

196 N. T. Fairweather, M. S. Gibson and H. Guan, *Organometallics*, 2015, **34**, 335–339.

197 T. Zell, Y. Ben-David and D. Milstein, *Angew. Chem., Int. Ed.*, 2014, **53**, 4685–4689.

198 S. Chakraborty, H. Dai, P. Bhattacharya, N. T. Fairweather, M. S. Gibson, J. A. Krause and H. Guan, *J. Am. Chem. Soc.*, 2014, **136**, 7869–7872.

199 E. Alberico, P. Sponholz, C. Cordes, M. Nielsen, H.-J. Drexler, W. Baumann, H. Junge and M. Beller, *Angew. Chem., Int. Ed.*, 2013, **52**, 14162–14166.

200 S. Werkmeister, K. Junge, B. Wendt, E. Alberico, H. Jiao, W. Baumann, H. Junge, F. Gallou and M. Beller, *Angew. Chem., Int. Ed.*, 2014, **53**, 8722–8726.

201 C. Bornschein, S. Werkmeister, B. Wendt, H. Jiao, E. Alberico, W. Baumann, H. Junge, K. Junge and M. Beller, *Nat. Commun.*, 2014, **5**, 4111.

202 F. M. A. Geilen, B. Engendahl, M. Hölscher, J. Klankermayer and W. Leitner, *J. Am. Chem. Soc.*, 2011, **133**, 14349–14358.

203 T. vom Stein, M. Meuresch, D. Limper, M. Schmitz, M. Hölscher, J. Coetzee, D. J. Cole-Hamilton, J. Klankermayer and W. Leitner, *J. Am. Chem. Soc.*, 2014, **136**, 13217–13225.

204 S. Qu, H. Dai, Y. Dang, C. Song, Z.-X. Wang and H. Guan, *ACS Catal.*, 2014, **4**, 4377–4388.

205 X. Yang, *ACS Catal.*, 2012, **2**, 964–970.

206 F. Hasanayn and A. Baroudi, *Organometallics*, 2013, **32**, 2493–2496.

207 H. Li, M. Wen and Z.-X. Wang, *Inorg. Chem.*, 2012, **51**, 5716–5727.

208 S. Takebayashi and S. H. Bergens, *Organometallics*, 2009, **28**, 2349–2351.

209 K. Junge, B. Wendt, H. Jiao and M. Beller, *ChemCatChem*, 2014, **6**, 2810–2814.

